Universiteit Utrecht

Institute for Theoretical Physics

Master Thesis

Magnetic Catalysis in Holographic QCD

Author:
Georgios Papadomanolakis
BSc

Supervisors:
Dr. Umut Gürsoy

A thesis submitted in partial fulfilment of the requirements for the degree of Master of Science

October 2014

Abstract

In this thesis we study, by using the AdS/CFT correspondence, the formation of a chiral condensate and the subsequent dependence on an external magnetic field in large N_c QCD-like theories at finite temperature. This was done via two gravity duals, the AdS-soliton model and the Improved Holographic QCD model to which a flavour sector was added by introducing probe branes. In the case of the AdS-Soliton, a 6 dimensional model with one spatial dimension compactified on a circle, a constructive effect on the condensate was observed, a phenomenon coined "Magnetic Catalysis". The second model proved to be substantially more difficult, failing to give the desired chiral symmetry breaking solutions due to numerical errors. Therefore an extensive discussion and outlook will be given in order for future work to be able to overcome this problems.

Contents

1 Introduction

Since its formulation Quantum Chromodynamics (QCD) has been the focus of both theory and experiment due to a significant number of peculiarities. As a strongly coupled theory exhibiting confinement and asymptotic freedom it proved increasingly challenging to describe it using our conventional methods, such as perturbation theory. Alternative methods like Lattice QCD were tried with varying success. Then Maldacena in 1997 conjectured the AdS/CFT correspondence[2] opening an entire new field with the potential to accurately describe strongly coupled theories.

One of the unique aspects of QCD, belonging to the non-perturbative regime, is the deconfinement crossover which becomes a first order phase transition in the limit of vanishing quark masses and the formation of the Quark Gluon Plasma(QGP) at extreme conditions. This phase transition is intrinscally coupled to a second phase transition, the chiral symmetry breaking phase transition and the subsequent forming of a quark antiquark condensate. When an external magnetic field is applied this condensate has been shown to exhibit non trivial dependence on the magnetic field. Based on perturbative techniques one would expect the condensate to be enhanced by the magnetic field but recent Lattice QCD studies suggest that, for temperatures close to the deconfinement temperature, the magnetic field can act destructively. The subject of this thesis is to study this dependence of the condensate on the magnetic field in two distinct holographic duals of QCD.

In Chapter 1 we give the reader an elementary introduction into our current understanding of QCD. This includes a field theoretical introduction to QCD with special focus on the chiral symmetry and a review of recent developments in the field of Lattice QCD. In Chapter 2 we present the AdS/CFT gauge/gravity duality and its extension to QCD-like theories. In Chapter 3 we review the holographic models which were used with the corresponding results being presented in Chapter 4. Finally a complete Discussion is given followed by an extensive Outlook summarising potential extensions and improvements of the project.

2 Quantum Chromodynamics and the Quark Gluon Plasma

2.1 An Elementary Introduction to QCD

Within the well established Standard Model the interactions between quarks and gluons, the basic constituents of matter, are mediated by the strong force. From a theoretical point of view it is described by an $SU(3)$ non-abelian gauge theory with gluons as the gauge fields and the quarks carrying a "colour" charge under the gauge group. With these properties the Lagrangian of the gauge theory is of the Yang-Mills form with an additional matter component dictated by the Dirac equation[1]:

$$\mathcal{L}_{QCD} = \bar{\psi}(i\gamma^\mu D_\mu - m)\psi - \frac{(F^a_{\mu\nu})^2}{4}, \tag{2.1}$$

where the gauge fields A^a_μ are in the adjoint representation with a as the generator index of the $SU(3)$ group and the fermions ψ are in the fundamental representation of the gauge group. The field strength is defined as:

$$F^a_{\mu\nu} = \partial_\mu A^a_\nu - \partial_\nu A^a_\mu + g f^{abc} A^b_\mu A^c_\nu, \tag{2.2}$$

with f^{abc} being the structure constants of the gauge group. Finally the covariant derivative is given, using the generating matrices of the group, as:

$$D_\mu = \partial_\mu - igA^a_\mu t^a. \tag{2.3}$$

Quantum Chromodynamics possesses two additional properties which make it stand out against the other physical theories.

Asymptotic Freedom Firstly as a non-abelian gauge theory with matter in the fundamental representation it exhibits *Asymptotic Freedom*. This implies that at increasingly high energies the coupling constant becomes weaker. In the case of an $SU(N_c)$ gauge theory with N_f species, or flavours, of quarks the beta function is given by

$$\beta(g) = -\frac{g^3}{16\pi^2}(\frac{11N_c}{3} - \frac{2N_f}{3}). \tag{2.4}$$

Due to the minus sign increasing the energy scale implies reducing the coupling constant yielding asymptotic freedom. Associated with the running of the β-function comes the typical energy scale, Λ_{QCD}, below which the next, low energy, characteristic property of QCD sets in.

Confinement At strong coupling constant values the theory has been shown, by putting it onto a Euclidean lattice, to only allow asymptotic states which are singlets under the color group $SU(3)$ [6]. This property is called *confinement* and explains the spectrum of hadrons. Intuitively it can be imagined as follows.

When one separates a quark and an antiquark a flux tube of gauge field forms. This tube, depicted in Figure 1, has a fixed energy density and radius at strong coupling implying that by pulling them apart the energy of the pair will increase linearly with the seperation.

This property of QCD does not have an analytic proof but is generally considered true due to the absence of free quarks in nature[1]. As it is a consequence of strong coupling at low energies it is a non-perturbative result and hence one needs to consider alternative solving techniques. Below we will go deeper into those.

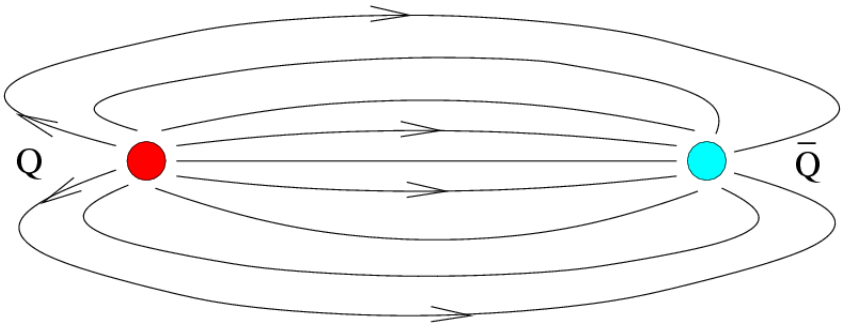

Figure 1: Gauge flux tube between a quark-antiquark pair.

2.2 The Chiral Symmetry

The gauge theory enhanced with matter possesses an additional symmetry besides the $SU(3)$ gauge symmetry, when one takes the quarks to be massless. This symmetry is called *Chiral Symmetry* and can be seen when one decomposes the quarks into left- and right-handed components[1].

To demonstrate the symmetry we consider QCD with two flavours. The matter lagrangian then becomes, in terms of left- and right-handed components:

$$\mathcal{L}_{matter} = \bar{u}_L i\not{D} u_L + \bar{u}_R i\not{D} u_R + \bar{d}_L i\not{D} d_L + \bar{d}_R i\not{D} d_R. \tag{2.5}$$

Writing the quark as a 2-dimensional vector

$$q = (u, d) \tag{2.6}$$

we obtain:

$$\mathcal{L}_{matter} = \bar{q}_L i\not{D} q_L + \bar{q}_R i\not{D} q_R, \tag{2.7}$$

which is invariant under transformations of the type $U(2)_R \times U(2)_L$. Decomposing into vector and axial parts we arrive at:

$$SU(2)_{L-R} \times SU(2)_{L+R} \times U(1)_{L-R} \times U(1)_{L+R}. \tag{2.8}$$

Here the vector symmetry $U(1)_{L+R}$ corresponds to the baryon number conservation. The other $U(1)$ symmetry does not correspond to a conserved quantity

as the corresponding current is not conserved due to a quantum anomaly. The remaining $SU(2)_{L-R} \times SU(2)_{L+R}$ gets broken to $SU(2)_{L+R}$, the *isospin*,when a chiral condensate $\langle \bar{q}_R q_L + \bar{q}_L q_R \rangle$ forms. We expect the chiral condensate to form as the attraction between quark and antiquarks is strong and hence creating a pair has a low energy cost.

The non zero expectation value for the chiral condensate indicates that the vacuum mixes the helicities of the quarks and, as dictated by Goldstone's theorem, one would expect three massless spin zero Goldstone bosons to be generated. In real life QCD massless particles do not exist but there is a triplet of light spin zero mesons, the pions. The pions have odd parity, consistent with a quark-antiquark pair, and satisfy the Gell-Mann-Oakes-Renner formula:

$$m_\pi^2 = (m_u + m_d)\frac{\sigma}{f_\pi^2}, \tag{2.9}$$

with σ the expectation value of the condensate for $m_u, m_d \to 0$ and f_π is the pio decay constant which can be fixed by the $\pi \to \gamma\gamma$ decay in QCD due to the electromagnetic anomaly.

To get the observed pion mass of 140 MeV the quark masses must be small, $(m_u + m_d) \approx 14 MeV$. This indicates that one can interpret the pion triplet as the pseudo-Goldstone bosons generated by the spontaneous breaking of an "approximate" chiral symmetry.

2.3 Magnetic Catalysis of Chiral Symmetry Breaking

We will now review the mechanism of chiral symmetry breaking under the influence of an external magnetic field. As we shall show the magnetic field enhances the symmetry hence the term "Magnetic Catalysis"[4].

We start from the action of a relativistic fermion in a four dimensional spacetime,

$$\mathcal{L} = \int d^4x \frac{1}{2}[\bar{\psi}(i\gamma^\mu D_\mu - m)\psi], \tag{2.10}$$

with the gauge field being

$$A_\mu^{ext} = -Bx_2\delta_{\mu,1}. \tag{2.11}$$

This system exhibits a very fundamental property due to the presence of the magnetic field. When one analyzes the spectrum it can be shown that it exhibits so called Landau levels

$$E_n(k_3) = \pm\sqrt{m^2 + 2|eB|n + k_3^2}, \quad n = 0, 1, 2.... \tag{2.12}$$

It is very clear that the levels are highly degenerate and parametrized by the momentum parallel to the magnetic field and a parameter n which, for large magnetic fields, encaptures the dynamics of the plane orthogonal to the magnetic field. Thus we see that effectively the system has been reduced to a $1+1D$ system, a phenomenon called *Dimensional Reduction*. The degeneracy factors are $|eB|/2\pi$ for the lowest level($n = 0$) and $|eB|/\pi$ for the remaining levels.

We now turn to the chiral symmetry breaking. The chiral condensate is defined through the Fermion propagator as

$$\langle 0|\bar{\Psi}\Psi|0\rangle = \lim_{x\to y} \mathrm{Tr}\, S(x,y). \tag{2.13}$$

Now the fermion propagator has the usual form

$$\begin{aligned} S(x,y) &= (i\gamma^\mu D^x_\mu + m)\langle x|\frac{-i}{(\gamma^\mu D_\mu)^2+m^2}|y\rangle \\ &= (i\gamma^\mu D^x_\mu + m)\int_0^\infty ds\langle x|e^{-is[(\gamma^\mu D_\mu)^2+m^2]}|y\rangle. \end{aligned} \tag{2.14}$$

The matrix elements can be computed by using Schwinger's proper time approach. The final result of this approach is given by

$$S(x,y) = e^{ie\int_y^x A^{ext}_\nu dx^\nu}\tilde{S}(x-y) \tag{2.15}$$

with

$$\begin{aligned} \tilde{S}(x) = -i\int_0^\infty \frac{ds}{16(\pi s)^2}\Big(& e^{-ism^2}e^{-(i/4s)[(x^0)^2 - x_A^2(eBs)\cot(eBs) - (x_3)^2]} \\ & (m + \frac{1}{2s}(\gamma^0 x^0 - \gamma^A x_A(eBs)\cot(eBs) - \gamma^3 x^3) - \frac{eB}{2}\epsilon_{AB}\gamma^A x^B) \\ & ((eBs)\cot(eBs) - \gamma^2\gamma^2(eBs))\Big), \quad A = 1,2,\ \epsilon_{12} = 1 \end{aligned} \tag{2.16}$$

We now transform to Euclidean momentum space ($k^0 \to ik_4, s \to is$) and we get our bilinear in the following form:

$$\begin{aligned} \langle 0|\bar{\Psi}\Psi|0\rangle &= \frac{-i}{(2\pi)^2}\,\mathrm{Tr}\int d^4k\tilde{S}_E(k) \\ &= \frac{4m}{(2\pi)^2}\int d^4k\int_{1/\Lambda}^\infty ds e^{-s(m^2+k_4^2+k_3^2+k_A^2(\tanh(eBs)/eBs)} \\ &= \frac{eBm}{(2\pi)^2}\int_{1/\Lambda}^\infty \frac{ds}{s}e^{-sm^2}\coth(eBs) \end{aligned} \tag{2.17}$$

with Λ the UV cutoff. Now lets expand the expression around an infinitesimal mass. This in order to understand the behaviour of the condensate for vanishing mass. Thus we acquire:

$$\langle 0|\bar{\Psi}\Psi|0\rangle = -|eB|\frac{m}{4\pi^2}(\Lambda^2 + |eB|\ln\frac{|eB|}{\pi m^2} - m^2\ln\frac{\Lambda^2}{2|eB|} + \mathcal{O}(m^4/|eB|)). \tag{2.18}$$

In the limit of zero mass we see that the condensate vanishes. Now, in the mean field approximation the gap equation for the dynamically generated mass has the form:

$$m = G\,\mathrm{Tr}\, S(x,x). \tag{2.19}$$

Combining the gap equation with the previously derived resut we arrive at the following mass gap formula:

$$m \simeq G\frac{m}{4\pi^2}\big(\Lambda^2 + |eB| \ln \frac{|eB|}{\pi m^2}\big). \tag{2.20}$$

This gap equation has a non trivial solution of the following form [4]:

$$m \simeq \sqrt{\frac{|eB|}{\pi}} \exp\big(\frac{\Lambda^2}{2|eB|}\big) \exp\big(-\frac{2\pi^2}{G|eB|}\big) \tag{2.21}$$

So we see that perturbatively the magnetic field enhances the dynamically generated mass, validating the term "Magnetic Catalysis".

2.4 The Quark Gluon Plasma

The theory of the strong force possesses an additional peculiarity. At extremely high temperatures and densities a new state of matter forms, the *Quark Gluon Plasma*. In this state the quarks and gluons are free and they are not constrained anymore to hadronic colour singlets. It is strongly believed that our universe was in the QGP state before hadronization. This makes the study of the QGP extremely important in the quest for understanding nucleosynthesis, the matter-antimatter asymmetry and so on.

After its postulation a long list of experiments were conducted in order to create this new state of matter. This lead to CERN announcing its discovery at the Super Proton Synchrotron(SPS) in 2000. Since then many experiments have been conducted in order to determine its properties at the Large Hadron Collider(LHC) in CERN and at the Relativistic Heavy Ion Collider (RHIC) in Brookhaven.

The most surprising property of the Quark Gluon Plasma was its strongly coupled nature which went against the paradigm of a weakly coupled QGP. This property became evident during non-central collisions of lead and gold nuclei ,at LHC and RHIC respectively. These collisions were done at large center of mass energies ($\sqrt{s} \approx 200GeV/$nucleon) in order to form a QGP for short timespans. Once it formes the QGP quickly hadronizes but as it turns out the pressure outwards is higher on the thin side. Consequently the detectors measured a higher flux of particles in the plane (elliptic flow) as can be seen in Figure 2a. This anisotropy then provides insight into the nature of the plasma. Now the property revealing the strongly coupled nature was the shear viscosity η of the plasma which was the lowest to be found in nature, Figure 2b!

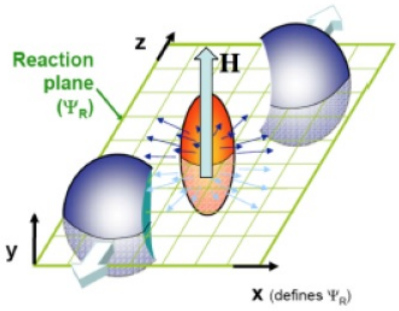

(a) The elliptic flow as a result of off-shell collisions. Here H is the induced magnetic field.

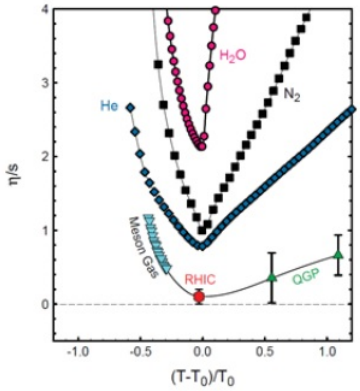

(b) The dimensionless shear viscosity of the QGP, H_2O, N_2 and He.

Figure 2

2.5 Lattice QCD

Due to the strongly coupled nature of QCD at low energies our most successful technique, perturbation theory, collapses and one needs to consider alternative techniques. The first alternative approach was constructed by K. Wilson who put QCD on a Euclidean lattice which he used to demonstrate confinement of quarks in his groundbreaking paper, published in 1974 [6]. Continuing along this line of thought it was shown that numerical results based on this approach could give quantitative results [7]. The significance of this gets enhanced by the fact it became possible to obtain quantitative results in strongly coupled domains thus enabling the studies of phenomena such as confinement, QGP and the deconfining phase transition.

The Setup

We start by introducing a four dimensional Euclidean lattice with size $N_\sigma^3 \times N_\tau$ and lattice spacing a. Therefore the volume and the temperature of the gauge theory can be linked to the number of points in the spatial and euclideanised time directions respectively by

$$V = (N_\sigma a)^3 \quad , \quad \frac{1}{T} = N_\tau a. \tag{2.22}$$

Having introduced the lattice one turns to the central entity of equilibrium field theory, the partition function, represented by a Euclidean path integral over the gluon and quark fields,

$$Z(V,T,\mu) = \int \mathcal{D}\mathcal{A}_\nu \mathcal{D}\bar{\psi}\mathcal{D}\psi e^{-S_E(V,T,\mu)}, \tag{2.23}$$

where A_ν and $\psi, \bar{\psi}$ obey periodic and antiperiodic boundary conditions respectively and the total Euclidean action consists of a fermionic and a gluonic part defined as follows

$$S_G(V,T) = \int_0^{1/T} \mathrm{d}x_0 \int_V \mathrm{d}^3\mathbf{x} \frac{1}{2}\mathrm{Tr}F^2$$
$$S_F(V,T,\mu) = \int_0^{1/T} \mathrm{d}x_0 \int_V \mathrm{d}^3\mathbf{x} \sum_{f=1}^{n_f} \bar{\psi_f} \not{D} \psi, \tag{2.24}$$

with n_f the number of quark flavours. The lattice spacing implies a natural momentum cut-off inversely proportional to a and therefore the theory is properly reguralized in the lattice formulation.

The discretization process now implies putting the fermions on the lattice sides and substituting the derivatives with finite differences,

$$\partial_\mu \psi_f(x) = \frac{\psi_{\hat{n}+\hat{\mu}} - \psi_{\hat{n}-\hat{\mu}}}{2a}. \tag{2.25}$$

Based on this it is natural to consider the gluonic fields to be placed on the links between neighbouring sites as they are the mediating particles of the theory. This requires the introduction of, so called, *link variables*

$$U_{x,\mu} = P \exp\Big(ig \int_x^{x+\hat{\mu}a} \mathrm{d}x^\mu A_\mu(x)\Big), \tag{2.26}$$

which describe the path ordered parallel transport of the gauge field from site x to site $x + \hat{\mu}a$. A product of the link variables around a closed lattice contour is called a Wilson loop which plays an integral part in Lattice QCD.

Firstly a Wilson loop around an elementary plaquette of the lattice can be used to reformulate the gauge invariant gluonic action up to errors of order $\mathcal{O}(a^2)$ giving the Wilson action. Secondly a Wilson loop around a closed contour is the appropriate quantity to show that theory exhibits confinement as Wilson showed in his paper. This characteristic of the Wilson loop will reappear in more detail at a later stage.

As a discretized version of a continuous theory it is essential for Lattice QCD to incorporate a smooth limit to the continuous case up to discretization errors of $\mathcal{O}(a^2)$. This is achieved by taking the lattice spacing to zero $a \to 0$. In order to keep the temperature $T = 1/N_\tau a$ consistently fixed it is necessary to take $N_\tau \to \infty$. Numerically this amounts to obtaining results for different lattice spacings and extrapolate those results to $N_\tau \to \infty$ at constant temperature.

Associated with the continuum limit comes a serious defect in the lattice approach. Due to the discretized derivative one obtains in the continuum limit a massless fermion propagator with more poles than just the zero momentum one. This leads to the "species doubling" problem. The mostly used approach to solving it is by considering staggered fermions, Dirac fermion components distributed over multiple sites. This reduces the degeneracy to four fermions and in the massless limit the chiral condensate is still the order parameter for the chiral phase transitions .

Numerical Approach and Technical Limitations

The formulation of QCD on a lattice acquired its full potential when one started to apply numerical methods in order to get quantitative results. This first one to do this was Creutz [7] , creating a new computational physics field dedicated to lattice QCD.

The numerical methods are dependent on the probability treatment of (2.23). To do this, one integrates out the fermionic degrees of freedom acquiring a path integral over the bosonic degrees of freedom with the determinant of the Dirac operator in some power playing the role of the statistical weight analogous to the Boltzmann weight [1]. One then can use Monte-Carlo methods to do quantitative calculations.

Powerful as these methods are they come with some subtleties which limit the regimes of QCD in which calculations are feasible.

- As the theory can be formulated purely on a Euclidean lattice one has to analytically continue to be able to calculate time dependent quantities. Till now no consistent analytic continuation has been constructed in order to be able to do non-equilibrium calculations.
- It is very natural to add a chemical potential term $\bar{\psi}\mu\gamma^0\psi$ to the Dirac operator. When one does this the determinant acquires a phase factor as the operator acquires complex eigenvalues and hence is not strictly positive. This implies failure of the statistical interpretation creating the so-called *sign problem*.

Results of Lattice QCD

Before moving on to an alternative methods of tackling QCD it is appropriate to document the progress made in this field due to the efforts of the Lattice QCD community with and without an external magnetic field[9],[8]. First we turn to the thermodynamics of QCD as it is the basis of our understanding of QCD. The most prominent entity when discussing thermodynamics is of course the free energy which is given by

$$\mathcal{F} = -\frac{T}{V}\ln Z. \tag{2.27}$$

Having found this quantity one can now calculate additional thermodynamic quantities. First of all the pressure p is simply minus the free energy. Now we can define:

- the energy density ϵ: $\frac{\epsilon-3p}{T^4} = T\frac{d}{dT}(\frac{p}{T^4})$,
- the entropy density s: $s = \frac{\epsilon+p}{T}$
- the sound velocity c_s: $c_s^2 = \frac{dp}{d\epsilon}$.

[1] I refrain from giving an explicit result as it is dependent on the way of solving the doubling problem.

In Figure 2.5 we show the behaviour of the dimensionless energy density, entropy density and pressure for a pure $SU(3)$ theory. We see that the curves approach the ideal gas limit as temperature increases. At $T/T_c = 1$ the appearance of a first order phase transition, the deconfinement phase transition, is evident.

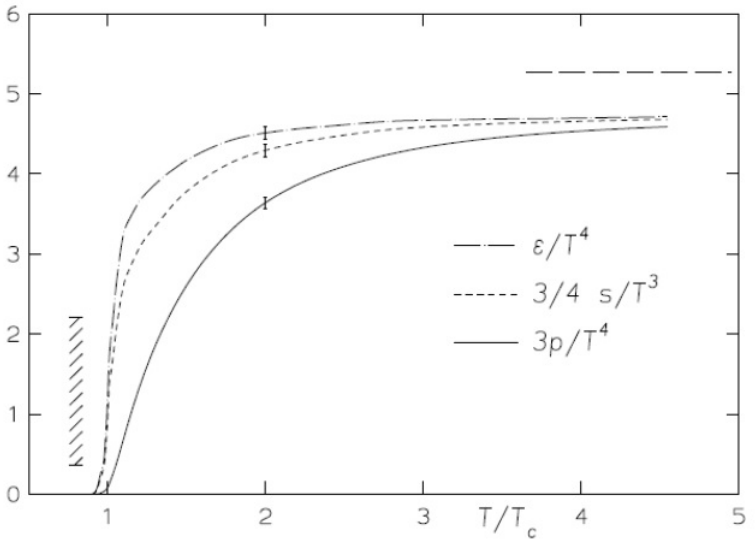

Figure 3: $SU(3)$ Thermodynamics. [8]

The deconfinement phase transition is the most significant physical phenomenon one can observe and is intrinsically connected to the symmetry breaking transition which is the main topic of this work, the chiral symmetry breaking. The connection arises when one considers confinement and the role it plays in the formation of a chiral condensate.

To study their connection one has to define the appropriate order parameters for the phase transitions. The parameters turn out to be the Polyakov Loop for the deconfinement phase transition and, as mentioned before, the chiral condensate for the chiral symmetry breaking,

$$\langle \bar{\psi}\psi \rangle = \frac{1}{N_\sigma^3 N_\tau} \frac{\partial}{\partial_m} \ln Z. \tag{2.28}$$

One can also look at the susceptibilities in order to determine the order of the phase transitions.

$$\chi_L = N_\sigma^3 (\langle L^2 \rangle - \langle L \rangle^2),\ \chi_m = \frac{\partial}{\partial_m} \langle \bar{\psi}\psi \rangle. \tag{2.29}$$

In Figure 2.5 the Lattice results for the suceptibilities have been plotted. From there one can determine that both transitions are continuous and lie very close

to each other with the critical temperature T_c around 160 MeV. It has to be mentioned that these results are not independent of the amount of flavours and the value of the quark masses taken into account. Especially the deconfinement phase transition is heavily influenced as it is intrinsically connected with the flavour degrees of freedom.

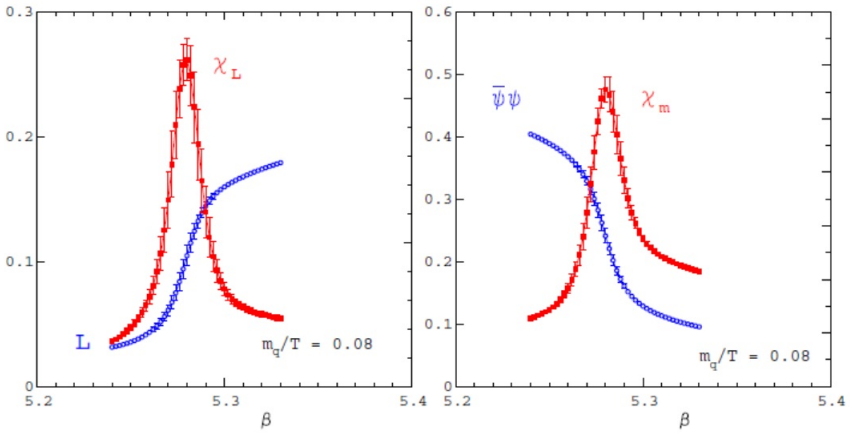

Figure 4: The Polyakov loop and the chiral condensate as a function of the coupling $\beta = \frac{6}{g^2}$. The corresponding susceptibilities show the transition points which are located at the peaks.[11]

The aforementioned influence of the flavours is being demonstrated in Figure 2.5 for multiple flavour combinations. Now one last comment can be made about the dependence of the pure glue part of the theory on the number of colours N_c. In Figure 3 we see that the energy and conformality measure points are almost indistinguishable when one increases the number of colours and also a very good fit with the Improved Holographic QCD model which will be discussed at a later stage. Thus it is clear that the role of N_c is small and thus can be chosen to be a convenient value. In the case of AdS/CFT, to be discussed in the next chapter, the number of colours is taken to infinity.

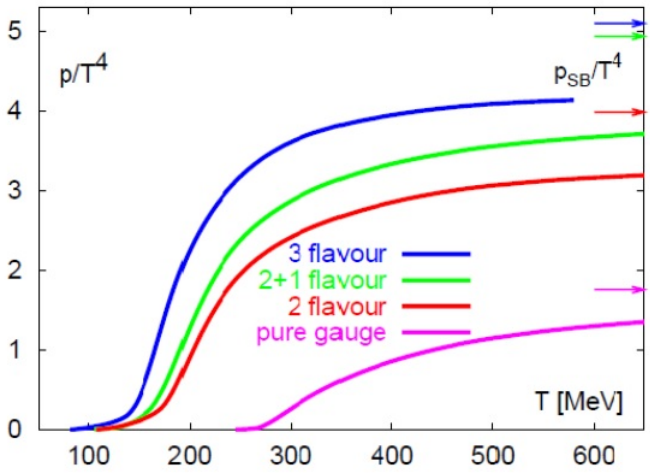

Figure 5: The dimensionless pressure for pure gauge and flavoured QCD.[11]

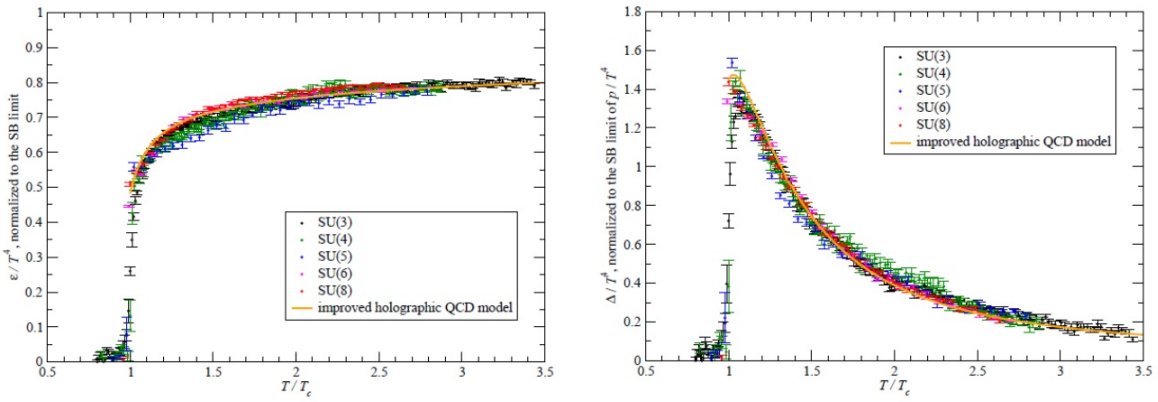

Figure 6: The dimensionless energy and conformal measure for lattice QCD models with different number of coulours N_c. The curve is the fitted Improved Holographic QCD model.[10]

Lattice QCD in an External Magnetic Field

Once the basic properties of QCD had been established through Lattice QCD it became increasingly important to consider additional effects. One of the most elementary additions would be to consider QCD under the influence of an external magnetic field [9]. A simple motivation would be the strong magnetic fields created during heavy ion collisions when one studies the QGP.

Here we will quickly present two phenomena stemming from the external

magnetic field. Firstly, related to the thermodynamics and the deconfinement phase transition of QCD, the dependence of T_c on the magnetic field was studied up to order $eB \sim 1GeV^2$, Figure 2.5. Two features show up during this study. Firstly the critical temperature decreases with increasingly strong magnetic field and secondly the order of the phase transition does not change under the influence of the magnetic field. The latter feature went against the established idea at that time.

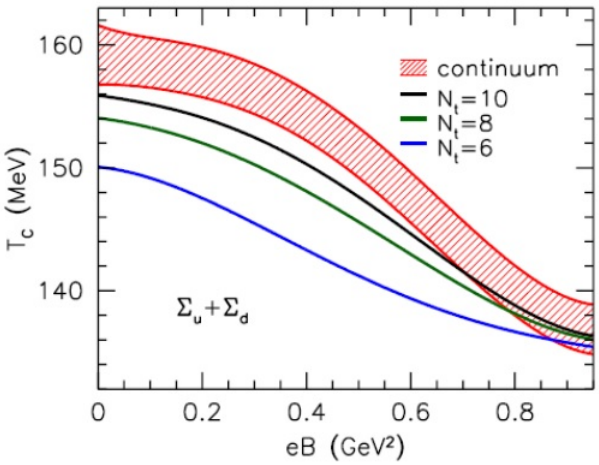

Figure 7: The critical temperature as a function of the magnetic field for 1+1+1 flavoured QCD.[9]

Furthermore the behaviour of the chiral condensate was studied in order to distinguish the influence of the magnetic field on the chiral symmetry breaking. The expectation, as discussed before, was that the magnetic field would act constructively to the condensate, a phenomenon coined "Magnetic Catalysis". This was indeed a result of the lattice study for $T = 0$ but at finite temperatures relatively close to the critical temperature an additional behaviour revealed itself. As can be seen in Figure 2.5 after a certain temperature there always is a value of the magnetic field beyond which it would act destructively to the condensate. This phenomenon is appropriatelly called *Inverse Magnetic Catalysis*.

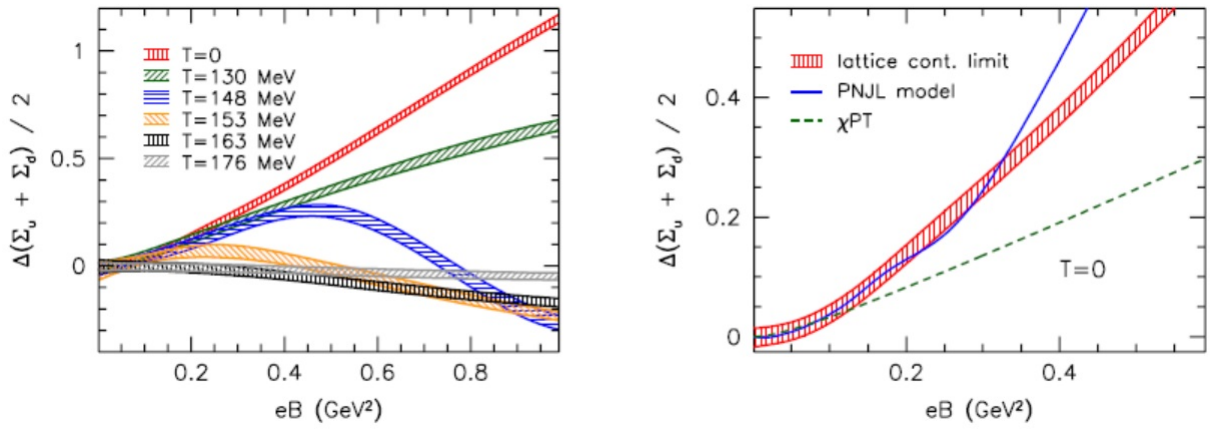

Figure 8: Left the behaviour of the normalized up and down chiral condensates for different temperatures. The Inverse magnetic catalysis happens at approximately $148MeV$. In the right Figure the $T = 0$ lattice result is compared to the results from chiral perturbation and the Nambu-Jona-Lasinio model.[9]

3 The AdS/CFT Gauge-Gravity Duality

Since the discovery of black holes the concept of holography has become an increasingly relevant subject within modern day high energy physics. The entropy of black holes was shown to scale as the area of its horizon instead of the volume as was expected, leading Prof. 't Hooft to conjecture the principle of holography [12] which afterwards was put into a string perspective by Susskind[13]. A precise description had to wait until 1997 when Juan Maldacena introduced, in his groundbraking paper[2], the AdS/CFT correspondence which, within the context of Type IIB string theory, links a gravitational theory in 5 dimensional AdS-space to a 3+1 dimensional $\mathcal{N} = 4SYM$ gauge theory living on the boundary of this space. The remaining five dimensions have been compactified on a sphere S^5. Formally this correspondence is captured in the following relation:

$$\langle e^{\int d^d x \phi_0(x)\mathcal{O}(x)} \rangle_{QFT} = Z_{string}\big(\phi(x,r)|_{\partial AdS} = \phi_0(x)\big) \tag{3.1}$$

where $\mathcal{O}(x)$ is an gauge invariant operator which has as a source, $\phi_0(x)$, the boundary value of a bulk field $\phi(x,r)$. Therefore this relation guarantees that one can obtain complete knowledge of the field theory, captured in the partition function, when the gravitational theory is completely understood and vice versa.

3.1 The Correspondence

The discovery the $AdS/$CFT correspondence was heavily influenced by the study of so-called p-branes. These objects are charged solitonic solutions to the classical equations of supergravity and can be seen as black holes extending in p spatial dimensions. In 1995 Polchinski [5] proved that another type of object, called a D_p-brane, gives the full string theoretical description of extremal p-branes ($Q = M$). This observation led to the final formulation of the correspondence.

Open strings can have two type of boundary conditions, Neumann and Dirichlet, with the latter one implying that the endpoints are confined to a hypersurface. These $p+1$ dimensional hypersurfaces are called D_p-branes. When one stacks N D_p-branes on top of each other the endpoints of the open strings are characterised by a Chern-Patton factor $|i\rangle$ that determines the D_p-brane on which the endpoint lies. Then open strings states will have labels of the type $\lambda^{\alpha}_{ij}|i\rangle|j\rangle$ and thus live in the adjoint of $U(N)$ as one can show that these are $U(N)$ matrices.

As the correspondence is valid in the supergravity limit of string theory we need to elaborate on this before continuing. The supergravity limit means that

- quantum string corrections which are governed by the string coupling $g_s = g^2_{YM}$ are supressed, $g_s \to 0$
- and the curvature of the background dominates over the string length hence $l = \sqrt{\alpha'}(g_s N)^{1/4} >> \sqrt{\alpha'} = l_s$. This implies that $g_s N >> 1$.

Thus the supergravity limit amounts to taking $g_s \to 0, N \to \infty$ while $\lambda = g_s N$ remains finite and large.

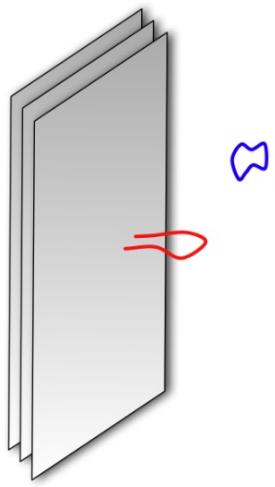

Figure 9: Stack of D3-branes[15].

Now consider a stack of N_c overlapping D_3 branes at infinity as in Figure 4. In the open string description the D_3-branes are viewed as the surfaces where the endpoints of open strings lie and the total string theory picture consists of:

- an open string sector living on the branes. One can show that the corresponding $U(N)$ theory reduces to $\mathcal{N} = 4$ Super Yang-Mills $SU(N)$ theory in the low energy limit.
- A closed string sector living in the bulk which reduces to supergravity in the low energy limit.
- The interaction between the two regimes. This interaction can be described as follows: two open strings can interact on the D_3-branes and merge to form a closed string. This will not be bounded to the branes and can propagate into the bulk.

The interaction action is proportional to $g_s\alpha'^2$ and hence the open and closed regimes become decoupled when one takes the limit $\alpha' \to 0$. This limit corresponds to the low energy limit of string theory which we already used in the other two regimes.

As the D_3 branes extend infinitely into the transversal directions their mass is infinite and hence they backreact on the system[2]. This mean that we can substitute them for their backreaction, the $3-$brane. Now the two decoupled regimes are

- At large distances, hence low energies as we have energy$\sim 1/$length, gravity becomes free. For the observer at infinity it amounts to massless particles propagating in the bulk with wavelengths that become very big. This is equivalent to closed strings propagating in 10 dimensional flat spacetime
- At small distances, from the point of view of the observer at infinity, all type of excitations that go close to $r \to 0$. The energy E_p measured at a point r is related to the energy measured at infinity through $E_p \propto rE$. so this implies that $r \to 0$ belongs to the low energy regime. Subsequently it can be shown that the geometry reduces to $AdS_5 \times S^5$ in this regime. The total spacetime then displays a "throat" structure, as shown in Figure 5, with the form of the throat being $AdS_5 \times S^5$.

As a final comment the decoupling of those two regimes can be seen as follows. The particles at large distances have a wavelengths much larger than the typical gravitational size of the brane and the particles close to the origin can not escape the gravitational potential, hence remaining in the asymptotic region.

[2]As a side note, the mass per unit p-volume, the tension, is finite and can be expressed as $T_{D_p} = \frac{1}{(2\pi)^p g_s l_s^{p+1}}$.

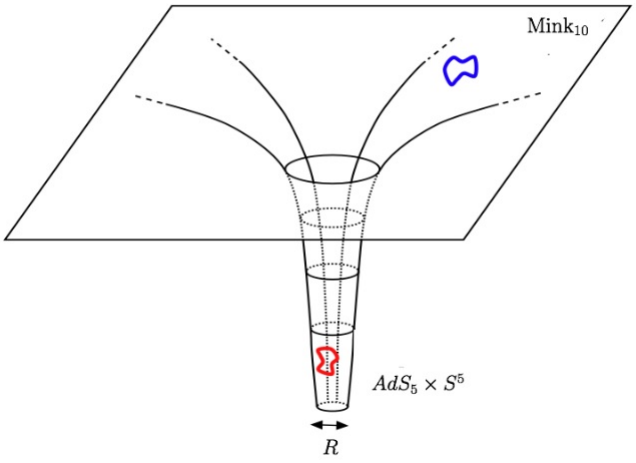

Figure 10: The spacetime formed by the backreaction of the D_3 branes which exhibits a "throat"[15].

Now one sees that both descriptions reduce to two decoupled theories in the low energy limit. In both cases one of the two systems is supergravity on flat space so we can conjecture that the other two theories are equivalent. This gives that *"$\mathcal{N} = 4$ $SU(N)$ SYM in 3+1 dimensions is dual to type IIB supergravity on $AdS_5 \times S^5$.*

Furthermore the AdS/CFT correspondence can also be shown to be a duality between a strong and weakly coupled theory. In an $SU(N)$ gauge theory 't Hooft showed that when one expands the partition function the 't Hooft coupling $\lambda = g^2_{YM}N$, for $N \to \infty$, suppresses all non planar diagrams[14]. As we saw before this approach is valid as the number of colours play a minimum role. Thus for the D-brane picture to be tractable one needs to take $\lambda << 1$ which is incompatible with the supergravity limit taken in the closed string picture. Therefore no contradiction arises and we see that the correspondence and perturbation theory apply in different regimes validating the term "duality". This makes the correspondence extremely useful as one can make calculations in the strongly coupled regime of gauge theories in which perturbation theory fails.

3.2 The Field Operator Correspondence

As already mentioned every field in the bulk is dual to an operator on the CFT side. This can be seen in the fundamental relation of AdS/CFT (3.1). This relation can be used to calculate correlation functions of the operator by the

usual method

$$\langle \mathcal{O}(x_1)...\mathcal{O}(x_n)\rangle = \frac{\delta^n}{\delta\phi_0(x_1)..\delta\phi_0(x_n)} Z_{string}\big(\phi(x,r)|_{\partial AdS} = \phi_0(x)/big)|_{\phi_0=0}. \tag{3.2}$$

The fundamental relation of AdS/CFT is valid in general, for any field.

Additionaly it turns out that there is a relation between the mass of each field and the scaling dimension of the gauge invariant conformal operator. In AdS_{d+1} space the wave equation of a field with mass m will yield two independent solutions, $r^{d-\Delta}$ and r^{Δ} when expanded near the boundary $r = 0$. Here the constant Δ is related to the mass by the equation

$$\Delta = \frac{d}{2} + \sqrt{\frac{d^2}{4} + R^2 m^2}. \tag{3.3}$$

Now the leading term of

$$\phi(r, x_\mu) = \phi_0(x_\mu) r^{d-\Delta} + \phi_1(x_\mu) r^{\Delta} \tag{3.4}$$

is singular for $\Delta > d$, vanishes for $\Delta < d$ and approaches a constant for $\Delta = d$. For a consistent description one needs to take the boundary condition

$$\phi(r, x_\mu) \to r^{d-\Delta}\phi(x_\mu). \tag{3.5}$$

ϕ itself is dimensionless hence ϕ_0 has dimension $d - \Delta$. Now the action $S = \int d^d x \phi_0 \mathcal{O}$ has to remain invariant under scaling transformations so the dimension of the operator $\mathcal{O}$ turns out to be Δ. One can also confirm that this is the correct conformal dimension of $\mathcal{O}$ by deriving the corresponding correlation function from (3.1) by plugging in the solution for the field (3.5).

3.3 Deforming the AdS/CFT Correspondence

Up till now the AdS/CFT correspondence has been presented within the context of a conformal boundary theory without temperature. For the correspondence to potentially describe realistic theories one needs to move away from conformality and deform the AdS gravity bulk. This must be done in order to incorporate certain elements which introduce scales into the boundary theory such as temperature and an energy scale related to the RG flow of the boundary theory.

The inclusion of temperature into pure AdS space can be done in two different ways. One can Euclideanize the pure AdS metric giving a so called "Thermal AdS" metric which has arbitrary temperature. The second way is by introducing a black hole in the AdS background. This black hole then has a Hawking temperature dependent on the radius of the horizon which one can derive by the familiar Euclideanization procedure. These two phases are separated by a so called "Hawking-Page" phase transition. Up to a certain temperature T_c the thermal AdS dominates as it has the lowest free energy. At that point a PT occurs and the black hole becomes the dominant solution. As the temperature in the bulk corresponds to the temperature measured at infinity, it corresponds to the temperature of the boundary theory.

Bulk/Gravity	**Boundary/Field Theory**
Metric tensor $g_{\mu\nu}$	Energy momentum tensor $T_{\mu\nu}$
Scalar field ϕ	Scalar operator $\mathcal{O}$
Dirac field ψ	fermionic operator $\mathcal{O}_f$
Gauge field A_μ	Global symmetry current J_μ
Mass of the field	Conformal dimension of the operator
Hawking temperature	Temperature
Local isometry	Global spacetime symmetry

Table 1: The Holographic Dictionary.

From the original setup up till now the role of the extra dimension has remained elusive. As it is a quantity of the bulk it should correspond to a quantity in the boundary theory and a study of the conformal group reveals that it is dual to the energy scale of the field theory. This implies that the limit $r \to 0$ corresponds to the UV completed theory and, more generally, moving along the radial dimension implies moving along the RG-flow of the boundary theory. If one introduces a cut-off or, as we will see later, a scalar dilaton field the RG-flow obtains a characteristic energy scale and hence conformality is broken. This is useful as QCD, for example, is a theory with a mass gap and a characteristic energy scale Λ_{QCD}.

Once the radial dimension has been related to the RG flow in the boundary theory one can list the most important bulk-boundary identifications. This is called the "Holographic Dictionary" and a part of it is shown in Table 1.

3.4 Wilson Loops

When discussing Lattice QCD a fundamental quantity appeared, the Wilson loop. It was defined in the context of discretized spacetime but it can be generalized to any field theory as follows. For every closed contour C and representation R of the gauge group the Wilson loop is given by[3]:

$$W_R(C) = \mathrm{Tr}_R \, P e^{i \int_C A_\mu^\alpha T^\alpha dx^\mu}. \tag{3.6}$$

It is the path integral of the holonomy of the gauge field along the contour with T^α the generators in R. One can see this as the introduction of a particle-antiparticle pair in the representation R with the contour being their path from their creation to their annihilation with the Wilson loop measuring the free energy of the state.

As mentioned at an earlier stage, the Wilson loop played an integral role in the discovery of confinement by Wilson. We shall now exhibit its role and demonstrate how the Wilson loop can be modeled through AdS/CFT.

In a confining theory, say QCD, external quarks have an energy which grows linearly with distance

$$E = m_q + m_{\bar{q}} + \tau L \tag{3.7}$$

hence there is a constant force pulling the quark to each other. Here τ is the QCD string tension. The QCD string is a confining colour flux tube which is an effective description in order to model confinement as seen before in Figure 1. The linear dependence on the distance implies that for two static quarks, which are modeled by a rectangular loop, the Wilson loop should go as follows:

$$W(C) = e^{-T\tau L} \propto e^{-\tau A(C)} \tag{3.8}$$

where $A(C)$ is the area of the loop and T the elapsed time. Confinement is a part of the glue vacuum as the the quarks were considered as external non dynamical sources.

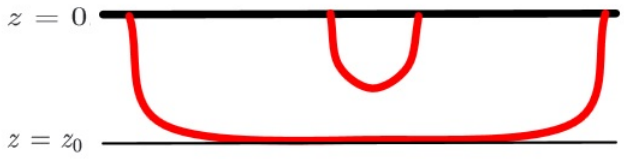

Figure 11: String configuration of the Wilson loop in the presence of a thermal gas[15].

On the AdS side of the story it is necessary to define an analogous quantity. A natural entity would be a string whose endpoints lie on the contour $\mathcal{C}$. This string is governed by the Nambu-Goto action $\int dx^2\sqrt{h}$ and hence wants to minimize its action by extending into the bulk. If the boundary theory is confining one would expect the following:

$$TE(L) = S_{NG}\big(X^{\mu}_{min}(\sigma,\tau)\big). \tag{3.9}$$

It can be shown that in conformal coordinates $ds^2 = e^{2A_s(r)}\eta_{\mu\nu}$ with $A_s(r) = A(r) + \frac{2}{3}\phi(r)$ the Wilson loop has the exact form as in equation (3.8) when A_s has a minimum at a point $r_\star$. The location of this minimum is the turning point of the string and we have that if $L \to \infty$ then $r \to r_\star$ (Figure 6). It follows that this configuration yields the required behaviour for confinement

$$W(C) = e^{TLe^{2A_s(r_\star)}}. \tag{3.10}$$

The above assumes that A_s is analytic and holds for zero temperature but can be easily generalized to arbitrary temperature. Using this description of confinement one can now easily see that the black hole phase in the AdS bulk corresponds to a deconfined phase as the string will sit on the horizon as can be seen in Figure 3.4. In the previous discussion this amounts to A_s not possessing a minimum in the presence of a black hole.

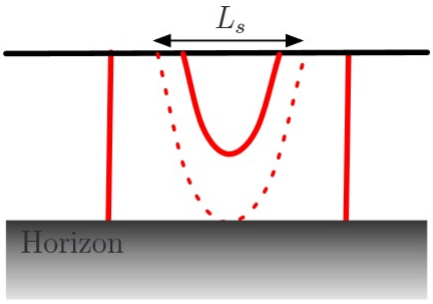

Figure 12: The string configuration for the Wilson loop in the presence of a black hole[15].

3.5 Matter in the Fundamental Representation

Adding matter in the fundamental representation, the flavour sector of QCD, to the boundary theory implies adding single lines to the 't Hooft expansion. Topologically this corresponds to adding boundaries to the Riemann surfaces in terms of which the 't Hooft expansion can be expressed[14] and within the context of AdS/CFT this is dual to adding boundaries to the worldsheet expansion in the bulk [17]. As boundaries are induced by an open string sector in the bulk one needs to add N_f overlapping D_p-$\bar{D}_p$-branes in the bulk, Figure 3.5. This can be achieved quite easily in the limit $N_f << N_c$ where the backreaction of the flavour branes can be neglected.

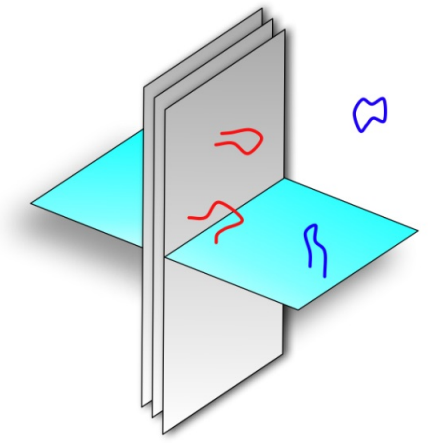

Figure 13: The flavour brane implementation in the bulk[15].

With the additional branes the open strings can have three different configurations regarding the location of their end points, namely $3-3$,$p-p$ or $3-p$. The coupling constant of an open string with both end points on a D-brane is given by $g_D \propto E^{(p-3)}$ and thus at low energies the $p-p$ open strings in the bulk decouple for $p > 3$ which is the case generally taken. The $3-p$ strings will interact with the $p-p$ and $3-3$ strings living on the D_p and D_3 branes respectively, with the corresponding coupling constants. Thus it follows that at low energies only the interactions with the $3-3$ strings survive. The vanishing of the effective coupling on the D_p branes additionally implies that the gauge group $SU(N_f)$ becomes a global symmetry group, the flavour symmetry group.

Now we proceed in a similar way as before by looking at two equivalent descriptions of the D_3/D_p system. In the $g_s N_c << 1$ case we have the system of D_3/D_p branes which reduces to two decoupled systems in the low energy limit. The first sector is free and consists of closed strings and $p-p$ open strings propagating in ten dimensional flat space-time and on the worldvolume of the flavour branes while the second is a $\mathcal{N} = 4$ SYM coupled to the flavour degrees of freedom. These additional degrees of freedom transform in the fundamental representation of both the $SU(N_c)$ gauge group and the $SU(N_f)$ global, flavour, symmetry group.

Now in the $g_s N_c >> 1$ case we study the same system from the closed string point of view so we can study the D_3 branes by looking at their backreaction. This will give again two decoupled systems in the low energy limit, closed strings and $p-p$ open strings propagating in ten dimensional flat spacetime and an $AdS_5 \times S^5$ "throat" containing the flavour branes, Figure 7.

As done before we compare the two descriptions in the two different sectors in the low energy limit. Again the two regimes possess a free sector of propagating closed strings and $p-p$ open strings in flat spacetime hence leaving us to identify the other two sectors. So we conjecture that *"$\mathcal{N} = 4$ SYM coupled to N_f flavours of fundamental degrees of freedom is dual to type IIB closed strings in $AdS_5 \times S^5$, coupled to open strings propagating on the worldvolume of N_f D_p-branes and $\bar{D}_p$-antibranes."*

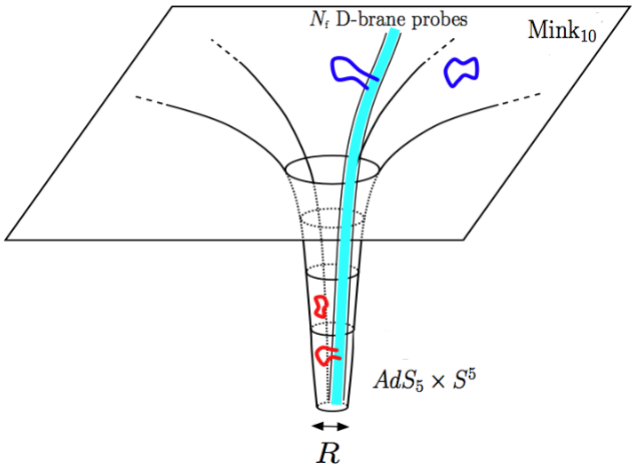

Figure 14: The modified "throat" containting the probe branes[15].

We conclude this chapter by giving and discussing the action for the N_f overlapping flavour branes and antibranes proposed by Sen [18]. This semi-classical action is a generalization of the usual DBI-action and includes the dynamics of the lowest open string mode, the tachyon. The action reads:

$$S = -\int d^{p+1}x \mathbf{STr}[e^{-\phi}V(TT^\dagger, Y_L^I - Y_R^I, x)(\sqrt{-\det \mathbf{A}_L} + (\sqrt{-\det \mathbf{A}_R})] \quad (3.11)$$

where **STr** is the symmetric trace as defined in [31] and the fields are:

$$A_{(i)MN} = g_{MN} + B_{MN} + F^{(i)}_{MN} + \partial_M Y^I_{(i)} \partial_N Y^I_{(i)} + \frac{1}{\pi}(D_M T)^*(D_N T) + \frac{1}{\pi}(D_N T)^*(D_M T)$$
$$F^{(i)}_{MN} = dA^{(i)} - iA^{(i)} \wedge A^{(i)}, \quad D_M T = (\partial_M + iA^L_M - iA^R_M)T. \quad (3.12)$$

We have set $2\pi\alpha' = 1$ and $V(\tau^2, Y^I_L - Y^I_R, x)$ is the tachyon potential. In the rest of this thesis the transverse scalars $Y^I_{L/R}$ and the B-field will be set to zero as they have no analogue in QCD. Additionally there is an extra contribution coming from the WZ coupling of the flavour branes with the RR potentials which is given by the following action

$$S_{WZ} = T_p \int_{\Sigma_{p+1}} C \wedge \mathbf{Str} e^{i2\pi\alpha' \mathcal{F}} \quad (3.13)$$

where Σ_{p+1} is the world volume of the branes, C is a formal sum of the RR potentials and $\mathcal{F}$ is the curvature of a superconnection $\mathcal{A}$ which can be expressed as follows

$$i\mathcal{A} = \begin{pmatrix} iA_L & T^\dagger \\ T & iA_R \end{pmatrix} \quad i\mathcal{F} = \begin{pmatrix} iF_L - TT^\dagger & DT^\dagger \\ DT & iF_R - TT^\dagger \end{pmatrix} \quad (3.14)$$

The superconnection is defined as

$$\mathcal{F} = d\mathcal{A} - i\mathcal{A} \wedge \mathcal{A} \tag{3.15}$$

and satisfies the Bianchi identity:

$$d\mathcal{F} - i\mathcal{A} \wedge \mathcal{F} + i\mathcal{F} \wedge \mathcal{A} \tag{3.16}$$

Now lets briefly review the appearance of the lowest string mode, the tachyon. The tachyon transforms in the bifundamental of $U(N_f)_L \times U(N_f)_R$ and therefore is the natural candidate for the chiral condensate which describes chiral symmetry breaking. As shown in [30] in a confining background whith no blackholes the tachyon must diverge in the deep IR region of the bulk. Intuitively this can be seen as a recombination of the branes and antibranes as they are not allowed to extend freely till the end of space. Mathematically it was shown that the tachyon must diverge in order for the WZ-sector to reproduce the correct field theory global anomaly. In agreement with the AdS/CFT dictionary the renormalizable component of the tachyon close to the boundary is dual to the bare quark mass while the non-renormalizable component is the quark bilinear of dimension three.

A last comment must be made concerning the limit we took. Up till now the flavour symmetry group was introduced by considering probe branes which do not backreact. An increasingly more relevant limit is the Veneziano limit where N_f/N_c is kept small but finite. The importance sits in the backreaction of the branes which can shed light on behaviours which do not appear when one neglects the backreaction. Of course the backreaction will make the system significantly more complex as one needs to solve the inhomogeneous Einstein Equations combined with the equation for the tachyon simultaneously. For this numerics are vital as analytically it seems improbable one can solve the system.

4 The Confining Holographic models

4.1 AdS-Soliton

4.1.1 The Model

The first methods of introducing confinement in the AdS/CFT correspondence were done consisted of introducing a hard wall in the IR region of the bulk with reflecting boundary conditions. A slightly more elegant way was introduced when solving the folowing action[32]:

$$S = \int d^6x \sqrt{g_{(6)}} \big(e^{-2\phi}(R + (4\partial\phi)^2 + \frac{c}{\alpha'}) - \frac{1}{26!}F_{(6)}^2\big) \tag{4.1}$$

with constant c. This admits a special solution which is a double Wick rotation or an AdS_6 Swartszchild black hole. This solution is called the AdS soliton with the following metric:

$$ds_6^2 = -g_{tt}dt^2 + g_{zz}dz^2 + g_{xx}dx_3^2 + g_{\eta\eta}d_\eta^2 = \frac{R^2}{z^2}\big(dx_{1,3}^2 + f_\Lambda^{-1}dz^2 + f_\Lambda d_\eta^2\big) \tag{4.2}$$

with

$$f_\Lambda = 1 - \frac{z^5}{z_\Lambda^5} \tag{4.3}$$

The active RR-form we consider is:

$$F_{(6)} = \frac{Q_c}{\sqrt{\alpha'}}\sqrt{-g_{(6)}}d^6x \tag{4.4}$$

where Q_c is a constant proportional to the number of colours. Finally the dilaton is constant and given by:

$$e^\phi = \frac{1}{Q_c}\sqrt{\frac{2c}{3}}. \tag{4.5}$$

As we have done a double Wick rotation the coordinate η is compactified and due to regularity at z_λ we have

$$\eta \sim \eta + \delta\eta, \qquad \delta\eta = \frac{4\pi}{5}z_\Lambda = \frac{2\pi}{M_{KK}}. \tag{4.6}$$

This geometry has a "cigar" form and ends smoothly in the IR at z_Λ. Initially it is dual to an 1+4 dimensional gauge theory compactified on a circle with antiperiodic boundary condition which break supersymmetry. Hence it reduces to a 1+3 dimensional confining theory coupled to Kaluza-Klein fields.

To obtain a theory with temperature we do the natural thing, compactify the time direction. Then it turns out there is a second solution competing with the soliton, the normal Swartszchild black hole with the following metric:

$$ds_6^2 = \frac{R^2}{z^2}\left(dx_3^2 + f_T^{-1}dz^2 - f_T d_t^2 + d\eta^2\right) \tag{4.7}$$

where

$$f_T = 1 - \frac{z^5}{z_T^5}. \tag{4.8}$$

After Euclideanizing we obtain the temperature of the black hole

$$T = \frac{5}{4\pi z_T}. \tag{4.9}$$

It is evident that when both solutions are Euclideanized they are related by the transformation $t_E \leftrightarrow \eta, z_T \leftrightarrow z_\Lambda$ and thus it is clear that a first order deconfining phase transition happens at

$$T_c = \frac{M_{KK}}{2\pi} = \frac{5}{4\pi z_\Lambda}. \tag{4.10}$$

Above T_c the black hole dual to the deconfining phase dominates while below the AdS-Soliton does.

4.1.2 The Tachyon

With the predetermined backgrounds in mind we turn to the topic of adding flavour in the quenched approximation. Here we consider a single pair of D_4 brane-antibrane which again will be given by the Sen action advocated earlier. In the string frame the expressions is the following:

$$S_DBI = -\int d^4xdzV(|T|)(\sqrt{-\det \mathbf{A}_L} + \sqrt{-\det \mathbf{A}_R}) \tag{4.11}$$

with

$$\begin{aligned} A_{(i)MN} &= g_{MN} + \frac{2\pi\alpha'}{g_V^2}F^{(i)}_{MN} + \pi\alpha'\lambda((D_MT)^*(D_NT) + (D_NT)^*(D_MT)). \\ D_MT &= (\partial_M + iA^L_M - iA^R_M)T \end{aligned} \tag{4.12}$$

The indices M, N run over the worldvolume dimensions while μ, ν stand for the usual Minkowski directions. The complex tachyon is defined as $T = \tau e^{i\theta}$ and two constants, g_v and λ have been included which define the normalisation of the fields. Finally we need for our construction the tachyon potential which we take to be

$$V = \mathcal{K}e^{-\frac{1}{2}\mu^2\tau^2} \tag{4.13}$$

where $\mathcal{K}$ a constant which is related to the tension of the branes but drops out in all the calculations. For our purposes it suffices to look at the Sen action which includes the tachyon and a $U(1)$ gauge-field which will include the magnetic field necessary for magnetic catalysis. The resulting expressions reads:

$$\begin{aligned} S_{DBI} &= -2\mathcal{K}\int d^4xdze^{-\mu^2\frac{\tau^2}{2}}\sqrt{-\det[g_{\mu\nu} + \frac{2\pi\alpha'}{g_V^2}F_{\mu\nu} + (2\pi\alpha')\lambda\partial_\mu\tau\partial_\nu\tau]} \\ &= -2\mathcal{K}\int d^4xdze^{-\mu^2\frac{\tau^2}{2}}\frac{(g_{tt}g_{xx})^{1/2}}{g_V^2}\sqrt{(4B^2\pi^2\alpha'^2 + g_V^4g_{xx}^2)(g_{zz} + 2\pi\alpha'(\partial_z\tau)^2\lambda)} \end{aligned} \tag{4.14}$$

Here the gauge field is taken to be $A_\mu = (0, 0, yB, 0, 0, 0)$. As we take the branes in the probe limit no backreaction is generated hence the previously discussed background solutions still remain valid. They simply need to be substituted in the tachyon equation of motion in order to find the corresponding behaviour for the tachyon. Proceeding along this train of thought we vary with respect to the tachyon and obtain:

$$\begin{aligned} &\tau''(z) + \frac{\mu^2 g_{zz}\tau(z)}{2\pi\alpha'\lambda} + \frac{\tau'(z)}{2}(-\frac{g'_{zz}(z)}{g_{zz}(z)} + \frac{g'_{tt}(z)}{g_{tt}(z)} + \frac{g'_{xx}(z)}{g_{xx}(z)}\frac{4B^2\pi^2\alpha'^2 + 3g_V^4g_{xx}(z)}{4B^2\pi^2\alpha'^2 + g_V^4g_{xx}(z)}) + \mu^2\tau(z)\tau'(z)^2 \\ &+ \pi\alpha'\lambda\frac{\tau'(z)^3}{g_{zz}(z)}(\frac{g'_{tt}(z)}{g_{tt}(z)} + \frac{g'_{xx}(z)}{g_{xx}(z)}\frac{4B^2\pi^2\alpha'^2 + 3g_V^4g_{xx}(z)}{4B^2\pi^2\alpha'^2 + g_V^4g_{xx}(z)}) = 0 \end{aligned} \tag{4.15}$$

From now on we take $\mu^2 = \pi$ and we use the combinations $R = \sqrt{6\alpha'}$ and $\lambda^2 g_V^4 = \frac{2}{3}$ [32] in order to get rid of the constants and after using the metric

components we arrive at the final form which only depends on B:

$$\tau'' = -\frac{1}{6r}\Big(3\tau'\frac{-6(-6+r^5)+B^2\pi^2r^4(2+3\tau^5))}{(6+B^2\pi^2r^4)(-1+r^5)} + (\tau')^3\frac{4\pi r^2(12+B^2\pi^2r^4)(-1+r^5)}{6+B^2\pi^2r^4} + 6\tau\frac{-3+\pi r^2(-1+r^5)(\tau')^2}{r(-1+r^5)}\Big) \quad (4.16)$$

The UV-structure of the tachyon equation turns out to be independent of the magnetic field at leading order. This implies one can use the same near boundary expansion ($r \to 0$) for the tachyon as advocated in [30]:

$$\tau = c_1 r + \frac{\mu^2}{6}c_1^3 r^3 \ln r + c_3 r^3 + \mathcal{O}(r^5). \quad (4.17)$$

To arrive at this result $\frac{R^2\mu^2}{2\pi\alpha'\lambda} = 3$ was imposed. This was necesary in order to enforce that the bifundamental operator dual to the tachyon, with mass $m_\tau = \frac{-\mu^2}{2\pi\alpha'\lambda}$, has UV dimension 3 as we would expect from the quark bilinear $\bar{q}q$ in QCD. The correct dimension was obtained by using the mass-operator dimension correspondence conjectured at an earlier stage

$$\Delta(\Delta - 4) = m_\tau^2 R^2. \quad (4.18)$$

According to the holographic dictionary the source c_1 corresponds to the mass and the vev c_3 to the chiral condensate. The deep IR behaviour in the case of the soliton, which requires the tachyon to diverge in a very specific manner[32], and the regularity conditions at the horizon of the black hole relate those two quantities giving a dynamical dependence of the condensate on the mass. Now, in the case of the soliton without magnetic field, Kiritsis et. al. proceeded to determine the condensate as a function of the mass by shooting from the UV using (4.17) and matching to the appropriate IR-asymptotics which can be found in [32]. This gave the behaviour portrayed in Figure 8.

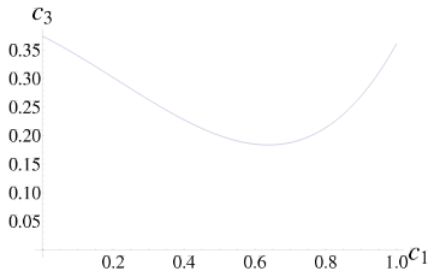

Figure 15: c_3 as a function of c_1 for $B = 0$ [32].

4.2 Improved Holographic QCD

4.2.1 Introduction

The AdS/CFT correspondence presented has its most precise form when one considers super symmetric conformal Yang-Mills theories. Now the essence of the practical use of the correspondence lies in deforming it so that it can be applied to realistic systems. As shown before (Ch. 2.2), this includes aspects like confinement and mass gap. In the case of modeling QCD one wants to apply holography while including phenomena where strong IR physics play a vital role. Besides confinement this includes chiral symmetry breaking and matching the spectra of baryons, mesons and their interactions.

A phenomenological approach called AdS/QCD was developed and has been applied with mixed success in mainly describing the meson sector. This approach is based on introducing an IR and UV cutoff with a constant dilaton. Confinement is imposed by specific IR boundary conditions at the IR cutoff.[20]

Continuing on the mostly phenomenological path, Kiritsis and collaborators [23] developed a more sophisticated approach which uses aspects of non-critical string theory as well. Specifically, an effective action is constructed based on understanding of string theory which then is matched to the phenomenological results we have of QCD. This approach is called "Improved Holographic QCD" and describes the glue sector of QCD.

In [21],[22],[25] it was shown that a Einstein-dilaton gravity system with a monotonic dilaton potential that grows fast enough is dual to a theory with the phase structure of a pure Yang-Mills field theory at large N_c. The theory possesses two phases, a thermal gas and a black hole, which correspond to the confining and deconfining phase transition respectively. At at a certain temperature a first order "Hawking-Page phase transition" occurs, dual to the confinement-deconfinement phase transition. Finally to include flavour degrees of freedom one considers the addition of branes as presented in the previous section based on the DBI-action proposed by Sen [18].

4.2.2 The Ingredients

The theory is determined by a set of parameters. They consist of the $5D$ Planck mass M_p and the parameters that define the dilaton potential $V_g(\lambda)$. The value of the potential for $\lambda = 0$ defines the AdS_5 length $\mathcal{L}_0$. These parameters will be fixed by matching to phenomenological and perturbative results.

The action ansatz for the Improved Holographic theory reads as follows:

$$S_5 = -M_p^3 N_c^2 \int d^5x\sqrt{g}\big(R - \frac{4}{3}(\partial\Phi)^2 + V_g(\Phi)\big) + 2M_p^3 N_c^2 \int_{\partial M} d^4x\sqrt{h}K, \quad (4.19)$$

with N_c the number of colours. The second term is the Gibbons-Hawking term which is necessary for a correct variation procedure[19], with K the extrinsic curvature of the boundary. The metric ansatz will be in the conformal coordi-

nates and has the form

$$ds^2 = e^{2A(r)}\big(-f(r)dt^2 + \frac{dr^2}{f(r)} + \eta_{ij}dxdx^j\big). \tag{4.20}$$

The dilaton $\lambda = e^{\Phi}$ is related to the 't Hooft coupling $\lambda_t = N_c g^2_{YM}$ up to a multiplicative factor which does not influence observables. The radial coordinate r corresponds to the RG scale of the boundary theory. Specifically we can identify the energy scale E with $A(r)$, the scale factor. This is done in the following way: $E = E_0 e^{A(r)}$.

With these matchings we can define the β-function within the holographic setup as follows:

$$\beta(\lambda) = \frac{d\lambda}{d\log E} = \lambda\frac{\dot{\Phi}}{\dot{A}}. \tag{4.21}$$

Having introduced the building blocks of Improved Holographic QCD one can start matching to phenomenology in order to model QCD. For complete analysis of this matching we refer the reader to [25],[24].

4.2.3 The Dilaton Potential

All the physics of the glue sector of QCD are encoded in the dilaton potential $V_g(\lambda)$ which up till now has not been specified. Its general form will be dictated by the IR- and UV-asymptotic form which will be matched in such a way to include confinement and asymptotic freedom. The matching will be done for the vacuum solution which contains a singularity in the deep IR($r \to \infty$). In conformally flat coordinates this gives:

$$ds^2 = e^{2A_0(r)}(dr^2 + \eta_{ij}dx^i dx^j), \quad \Phi = \Phi_0(r). \tag{4.22}$$

IR Asymptotics and Confinement In the IR the relevant physical phenomenon is confinement which implies that the Wilson loop yields an area law when the metric has the IR-asymptotic form. As shown in [23] this requires the potential to grow as $\lambda^{4/3}$ or faster. A second requirement is for the singularity in the deep IR to be a "good" singularity implying that it is repulsive to physical modes. "Bad" singularities allow physical mode to penetrate arbitrarily deep into the IR hence boundary conditions at the singularity are needed. This requirement, combined with confinement, yields the necessary IR asymptotic form for the potential:

$$V_g(\lambda) = V_\infty(\log\lambda)^{4/3}\lambda^{\frac{\alpha-1}{\alpha}} \tag{4.23}$$

with $\alpha \geq 1$ for confinement. The value of α can be fixed by demanding a linear glueball spectrum:

$$m_n \propto n^{(\alpha-1)/a} \tag{4.24}$$

Obviously this will give $\alpha = 2$.

UV Asymptotics and the β-function For the AdS/CFT correspondence to be valid the geometry must be asymptotically Anti-de Sitter. The addition of asymptotic freedom requires an logarithmically running coupling. To add this the dilaton potential will be matched to perturbative, pure glue, QCD β-function,

$$\beta \propto -b_0\lambda^2 - b1\lambda^3 + .. \tag{4.25}$$

The matching is achieved by requiring the following asymptotic form of the potential

$$V_g(\lambda) = \frac{12}{\mathcal{L}_0^2}(1 + u_0\lambda + u_1\lambda^2 + ...), \tag{4.26}$$

where $\mathcal{L}_0$ is the AdS length and the dimensionless parameters u_i must be matched to the β-function coefficients. The correct matching requires

$$u_0 = \frac{8b_0}{9}, \quad u_1 = \frac{4b_1}{9} + u_0^2\frac{828}{2304}. \tag{4.27}$$

With this UV asymptotic form of the potential the UV region in the conformal coordinates is given by:

$$\begin{aligned} e^{A(r)} &= \frac{l}{r}\big[1 + \frac{4}{9}\frac{1}{\log r\Lambda} - \frac{4}{9}\frac{\log(-\log r\Lambda)}{\log^2 r\Lambda} + ..\big], \\ b_0\lambda(r) &= -\frac{1}{\log r\Lambda} + \frac{b_1}{b_0^2}\frac{\log(\log r\Lambda)}{\log^2 r\Lambda} + .. \end{aligned} \tag{4.28}$$

Here the scale Λ is the only physical integration constant and can be holographically related to the strong coupling scale of QCD, Λ_{QCD}. One can determine the scale by a combination of initial conditions for the dilaton and the scale factor at a point r_0 close to the boundary,

$$\Lambda l = \exp A(\lambda_0) - \frac{1}{b_0\lambda_0}(b_0\lambda_0)^{-b_1/b_0^2} + .. \tag{4.29}$$

The extra contributions are subleading and vanish as one sends $\lambda_0 \to 0$.

The Final Ansatz for the Dilaton Potential In the literature, concerning Improved Holographic QCD and exponents of it, there are two ansatz which contain the necessary asymptotic behaviour but differ in the bulk and in the proportionality factor in the deep IR, V_∞. These are the following

- **Potential I [23]**

$$V_g(\lambda) = \frac{12}{\mathcal{L}_0^2}\big(1 + V_0\lambda + V_1\lambda^{4/3}\big(\log(1 + V_2\lambda^{4/3} + V_3\lambda^2)\big)^{1/2}\big), \tag{4.30}$$

  with $V_0 = u_0$, $V_1 = 14$, $V2 = \frac{u_1^2}{V_1^2}$ and $V_3 = 170$. $V1$ and $V3$ were fixed by considering the thermodynamics of large N_c YM [24].

- **Potential II [26]**

$$V_g(\lambda) = \frac{12}{\mathcal{L}_0^2}\big(1 + \frac{88\lambda}{27} + \frac{4619\lambda^2}{729}\frac{\sqrt{1+\log(1+\lambda)}}{(1+\lambda)^{2/3}}\big). \tag{4.31}$$

  Here the λ^2 term of the UV-asymptotic form is multiplied with a confinement factor. From here on, unless stated otherwise, the second potential will be considered as the dilaton potential.

4.2.4 Finite Temperature

The relevant solutions to this work are the ones including temperature. This implies taking a potential ansatz with the correct asymptotics and solve for finite temperature. Once again this is done by going to Euclidean signature and compactifying the Euclideanised time direction on a circle with period $\beta = \frac{1}{T}$. This construction admits two type of solutions analogous to the case studied by Maldacena [2]:

Thermal Gas The thermal gas can be achieved by Euclideanizing the vacuum solution (4.22). This corresponds to a gas of thermal excitations above the same vacuum and possesses all the properties of the vacuum solution such as confinement, linear glueball spectrum etc. The Thermal Gas can have arbitary temperature as there are no restrictions on the period of the compactified dimension.

Black holes These solutions have the familiar form in conformal coordinates:

$$ds^2 = e^{2A(r)}[\frac{dr^2}{f(r)} - f(r)dt^2 + dx_m dx^m], \quad \Phi = \Phi(r) \tag{4.32}$$

where $f(r)$ possesses a root which signifies the location of the horizon. In contrast to the thermal gas solution this corresponds to a deconfined phase as A_{string} does not posses a minimum which the Wilson loop test requires [23].
The black hole solutions posses two branches characterised by their stability. The big black hole branch is thermodynamically stable as the specific heat is positive:

$$c_v = T\frac{dS}{dT} > 0 \tag{4.33}$$

while the small black hole branch has a negative specific heat, hence is unstable (see Figure 9). This implies that the black hole solutions posses a minimum temperature T_{min} below which only the thermal gas exists. This is a necessary property of confining theories as will be seen below.

As we have seen, up till a temperature T_{min} the only existing solution is the thermal gas. It now remains to see what happens above this temperature. This

[3]This can be achieved due to the monotonic behaviour of λ and the fact it goes to zero in the UV and to infinity in the IR

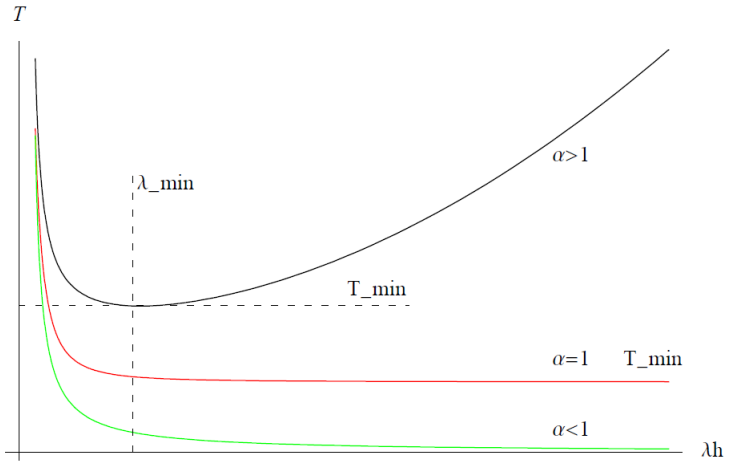

Figure 16: Temperature as a function of the horizon location[25]. The radial coordinate r has been replaced by the dilaton value at the horizon[3].

can be done by comparing the free energies(see Figure 4.2.4). Here we see that the black hole phase starts dominating above a temperature $T_c > T_{min}$ as the black hole free energy becomes smaller. At the transition temperature a first order phase transition occurs which is dual to the confinement/deconfinement phase transition of the boundary theory.

4.2.5 Adding Flavour

Having prepared the "glue" sector of the theory it is vital to add flavour in order to get closer to the physics of QCD and specifically the chiral symmetry breaking phenomenon. The addition proceeds along the lines of Ch. 3.5 as once again N_f branes and anti branes are taken[30]. In this model the branes will be overlapping D_4 branes with the Sen action reducing to[26]:

$$S = -\chi_f M_p^3 N_c^2 \int d^5x V_f(\lambda,\tau)\sqrt{\det(g_{\mu\nu} + \kappa(\lambda)\partial_\mu\tau\partial_\nu\tau + w(\lambda)F_{\mu\nu})} \qquad (4.34)$$

with $x = \frac{Nf}{Nc}$ determining the regime we sit in. For $\chi_f \to 0$ the quenched approximation is realized while χ_f finite signifies the Veneziano limit.

The potentials are chosen based on [29]. In their paper Kiritsis et. al. chose the potentials while considering the Veneziano limit, χ_f finite. The matchings proceed in a similar way as in the IHQCD case with a modified beta-function due to the added flavour which, up to two loops, is given by:

$$\beta^f(g) = -\frac{g^3}{(4\pi)^2}\left(\frac{11}{3}N_c - \frac{2}{3}N_f\right) - \frac{g^5}{(4\pi)^4}\left(\frac{34}{3}N_c^2 - \frac{N_f}{N_c}\left(\frac{13}{3}N_c^2 - 1\right)\right) \qquad (4.35)$$

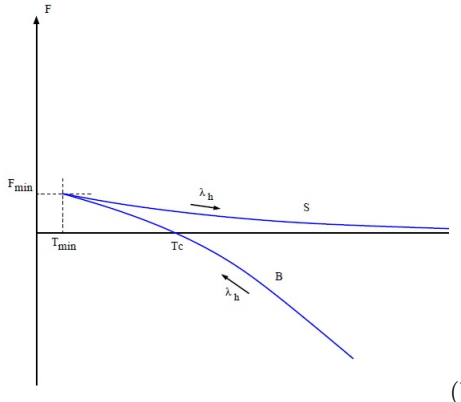

(a) Free energies of the two black hole branches [25].

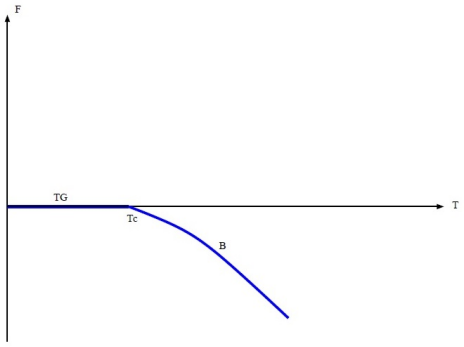

(b) Free energy comparison between the thermal gas and the big black hole branch[25].

Figure 17: The free energies of the Thermal gas and the different black hole branches.

and in terms of the dilaton λ:

$$\beta(\lambda) = -b_0\lambda^2 + b_1\lambda^3 + \mathcal{O}(\lambda^4) \tag{4.36}$$

with

$$b_0 = \frac{2}{3}\frac{11-2\chi_f}{(4\pi)^2}, \qquad \frac{b_1}{b_0^2} = -\frac{3}{2}\frac{34-13\chi_f}{(11-2\chi_f)^2}. \tag{4.37}$$

Additional constraints come from the behaviour of the tachyon. Firstly it has to decouple in the IR enforcing a specific form of the fermionic potential $V_f(\lambda,\tau) = V_{f0}(\lambda)e^{-\alpha(\lambda)\tau^2}$ and secondly the condensate $\bar{\psi}_L\psi_R$ has a perturbative anomalous dimension:

$$\gamma \equiv -\frac{d\ln m}{d\ln\mu} = \frac{a_0}{4\pi}g^2 + \frac{a_1}{(4\pi^2)^2}g^4 \tag{4.38}$$

$$\approx \frac{3}{(4\pi)^2}\lambda + \frac{203-10\chi_f}{12(4\pi)^4}\lambda^2 + \mathcal{O}(\lambda^3, N_c^{-2}). \tag{4.39}$$

In the second line the anomalous dimension is taken in the large N_c limit. These additional constraints combined with the IR constraint discussed at an earlier stage put additional constraints on the various potentials yielding the following selection:

$$V_f(\tau,\lambda) = W_0(1 + \frac{8(24+11W_0)}{27W_0}\lambda + \frac{20568+4619W_0}{729W_0}\lambda^2),\ \alpha(\lambda) = \frac{3}{2}, \tag{4.40}$$

$$\kappa(\lambda) = \frac{(1+\ln(1+\lambda))^\mu}{(1+\frac{3}{4}(\frac{115}{27}+\mu)\lambda)^{\frac{4}{3}}}, \quad w(\lambda) = \kappa(\lambda) \tag{4.41}$$

with μ taken to be $\mu = -\frac{1}{2}$

In the probe approximation the equations of motion reduce to a set of separate background equations of an Einstein-Dilaton background and a coupled system of equations for the Maxwell-Tachyon system. One then needs to find the background solution for the Einstein-Dilaton equation and subsequently introduce them into the Maxwell-Tachyon system which can then be solved. In the conformal coordinate system the background equations take the following form:

$$3A'' - 3A'^2 = -\frac{4}{3}\frac{\lambda'^2}{\lambda^2} \tag{4.42}$$

$$f'' + 3A'f' = 0 \tag{4.43}$$

$$3A'(f' + 4A'f) + V_g(\lambda)e^{2A} - f\frac{4}{3}\frac{\lambda'^2}{\lambda^2} = 0. \tag{4.44}$$

with the prime standing for the derivative w.r.t. the radial coordinate. By varying the action towards the dilaton one obtains its equation of motion. This equation does not provide new information as one can derive it from the previous three Einstein equations. Its form is:

$$f(\frac{\lambda''}{\lambda} - \frac{\lambda'^2}{\lambda^2}) + \frac{\lambda'}{\lambda}(f' + 3fA') = -\frac{3}{8}e^{2A}\partial_\lambda V_g. \tag{4.45}$$

Considering a gauge field sourcing a constant magnetic field

$$A_\mu = (0, By, 0, 0, 0) \tag{4.46}$$

the tachyon equation of motion becomes:

$$\begin{aligned}
&\tau'' - \frac{\partial_\tau \ln V_f}{\kappa}(e^{2A}/f + (\tau')^2\kappa) + (\tau')^3\kappa f e^{-2A}\Big(\frac{f'}{2f} + \frac{\lambda'}{2}\partial_\lambda \ln(\kappa V f^2) \\
&+ \frac{1}{2}\frac{8A'e^{8A} + B^2 w e^{4A}(4A'w + 2\lambda'\partial_\lambda w)}{e^{8A} + B^2 w^2 e^{4A}}\Big) \\
&+ \tau'\Big(A' + \frac{f'}{2f} + \frac{2A'e^{8A}}{e^8 A + B^2 w^2 e^{4A}} + \lambda'\partial_\lambda \ln(V_f\kappa) + \frac{\lambda' B^2 e^{4A} w^2 \partial_\lambda \ln w}{3^{8A} + B^2 w^2 e^{4A}}\Big) = 0.
\end{aligned} \tag{4.47}$$

5 Our Work

5.1 AdS-Soliton

The model containing an AdS-Soliton phase and a black hole phase, separated by a phase transition, provides an interesting playground in order to study magnetic catalysis as it is an improvement over the old soft- and hard-wall models. It is especially interesting to see if the inverse magnetic catalysis effect sets in at a high enough magnetic field. As we sit in the quenched approximation no backreaction of either the magnetic field or tachyon is considered. Thus the same background (4.2),(4.7) metrics can be used in the tachyon equation (4.16). The tachyon eom contains an explicit dependence on the magnetic field which will encode the magnetic catalysis effect. In the following we shall focus on the confining solution in the chirally broken phase. Reason for this is that it was shown in [32] that the deconfined phase, dual to the black hole, only admits a trivial solution for the tachyon when the quark mass is taken to be zero. Thus the black hole does not exhibit a chirally broken phase.

The goal is to solve the tachyon eom numerically by a shooting method. Firstly it is necessary to determine if the UV-asymptotics change on a leading level in order to get the correct condensate values. As this turns out to not be the case we can use the same UV-expansion as in the simple case (4.17). One then takes at a cutoff r_c^{UV} close to the UV the following boundary conditions for the tachyon and integrates up to the IR:

$$\tau(r_c^{UV}) = c_3(r_c^{UV})^3, \tag{5.1}$$

$$\tau'(r_c^{UV}) = 3c_3(r_c^{UV})^2 \tag{5.2}$$

where c_1 has been set to zero as the focus will be chiral symmetry breaking. Now in the IR it is necessary to match the solution to the correct asymptotic expansion. Following the methodology of [32] the tachyon is expressed as:

$$\tau(r) = \sum_{n=0}^{\infty}(r_\Lambda - r)^{(\frac{3(2n-1)}{20})}C_n g_n(r) \tag{5.3}$$

with the functions $g_n(r)$ having the following form:

$$g_n(r) = 1 + \sum_{m=1}^{\infty} D_{n,m}\Big(1 - \frac{r}{r_\Lambda}\Big)^m. \tag{5.4}$$

The constants are determined by plugging the ansatzë above in the tachyon equation (4.16) and solving order by order. We shall now give the first constants which still have a reasonabe size. Constants corresponding to higer orders have

been calculated as well but due to their size will not be given:

$$C_0 = C, \quad C1 = -\frac{26(9g_V^4\lambda^2 + B^2\mu^4)}{3C\mu^2(36g_V^4\lambda^2 + B^2\mu^4)} \tag{5.5}$$

$$C2 = -\frac{104(9g_V^4\lambda^2 + B^2\mu^4)^2(342g_V^4\lambda^2 + 29B^2\mu^4)}{9C^3\mu^4(72g_V^4\lambda^2 + B^2\mu^4)(36g_V^4\lambda^2 + B^2\mu^4)} \tag{5.6}$$

$$C3 = -\frac{104(9g_V^4\lambda^2 + B^2\mu^4)^3(2689200g_V^8\lambda^4 + 428328B^2g_V^4\lambda^2\mu^4 + 16921B^4\mu^8)}{81c^5\mu^6(36g_V^4\lambda^2 + B^2\mu^4)^3(2592g_V^8\lambda^4 - 108B^2g_V^4\lambda^2\mu^4 + B^4\mu^8)}. \tag{5.7}$$

Finally the first functions g_n are, again up till a manageable size, the following:

$$g_0(r) = 1 + \frac{3(54g_V^4\lambda^2 - 5B^2\mu^4)}{-360g_V^4\lambda^2 + 11B^2\mu^4} + \mathcal{O}(1 - \frac{r}{r_\Lambda}) \tag{5.8}$$

$$g_1(r) = 1 + \frac{18(-479196g_V^12\lambda^6 + 67176B^2b_V^8\lambda^4\mu^4 + 24891B^4g_V^4\lambda^2\mu^8 + 973B^6\mu^{12})}{13(468g_V^4\lambda^2 - 17B^2\mu^4)(360g_V^4\lambda^2 - 11B^2\mu^4)(9g_V^4\lambda^2 + B^2\mu^4)} + \mathcal{O}(1 - \frac{r}{r_\Lambda}). \tag{5.9}$$

This form of the tachyon close to the IR singularity can be seen as a "regularity condition" which relates the condensate to the mass in a non-trivial way. Also the constant C gets fixed by the mass.

Practically, the matching to the correct asymptotics can be done by eye. To be precise, a value of c_3 larger than the correct one will yield a solution which will diverge before the tip of the "cigar" and a value smaller will yield a finite solution. Therefore it was possible to find the condensate up to a high precision for increasing magnetic field. This result has been plotted in Figure 4.2.4 for $\mu^2 = \pi$ and $r_\Lambda = 1$ [4]. As one can see the condensate value monotonically increases, showing no sign of inverse magnetic catalysis.

[4]These choices are possible as we can always redefine the fields, $r \to \tilde{r} = r/r_\Lambda$ and $\tau \to \tilde{\tau} = \mu\tau$ leaving the tachyon equatio invariant.

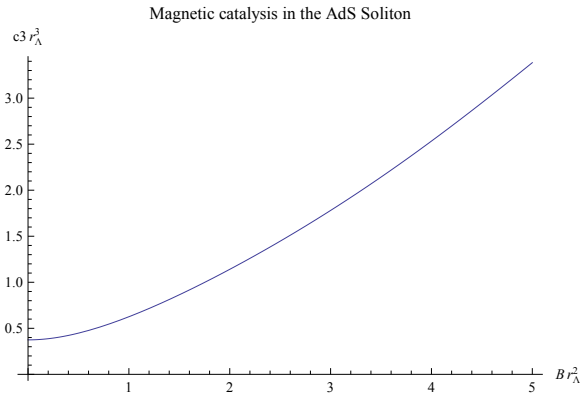

Figure 18: The dimensionless condensate plotted as a function of the dimensionless magnetic field

Now it is also possible to give the condensate in terms of the appropriate energy dimensions. This can be done by setting the appropriate length r_Λ which is equal to the inverse of Λ_{QCD}[32]. The result is show in Figure **??** where we chose the, approximately, correct physical value of $\Lambda_{QCD} = 300MeV$.

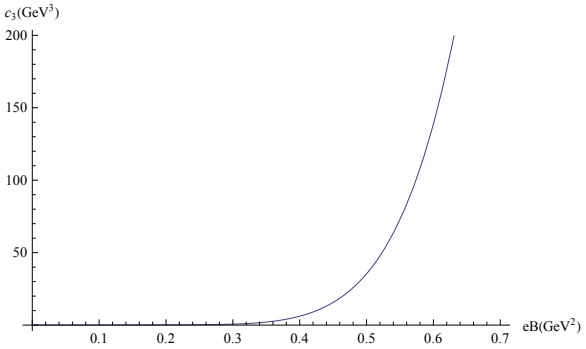

Figure 19: The dimensionful condensate plotted as a function of the magnetic field for $\Lambda_{QCD} = 300MeV$.

5.2 Improved Holographic QCD

After solving the tachyon eom in the presence of the AdS-Soliton background we turn to the more powerful QCD-dual, IHQCD. The ultimate goal remains the same, find a background solution while neglecting the flavour backreaction (quenched approximation) and consequently solve the tachyon eom coupled to a magnetic field in presence of the previously constructed background. The background solution constructed will be the confining one ($f = 1$) as we expect beforehand to witness chiral symmetry breaking. In the case of a deconfining, black hole, background a chirally broken phase was discovered only recently when considering the Veneziano limit[27],[28]. As the appearance of this phase was intrinsically connected to a non zero flavour to colour ratio $\chi_f = \frac{N_f}{N_c}$ it is improbable it would appear when this ratio is taken to be zero.

5.2.1 Solving the Background

As one proceeds to solve the set of Einstein equations (4.41) it is convenient to switch to a new coordinate system where the scale factor A plays the role of the radial component. This gives us the capability to penetrate arbitrarily deep into the UV and, as will become clear soon, it is necessary to penetrate up to $A \sim$ hundreds.

The transformation which will achieve the change of coordinates is given by:

$$q(A) = e^A \frac{dr}{dA}. \tag{5.10}$$

where $q(A)$ is a new function which goes asymptotically to $-\mathcal{L}_0$ in UV. The resulting Einstein equations are displayed in (A.2).

The construction of the background will be done numerically using an *ND-Solve* function in Mathematica. Now the main idea is to give boundary conditions deep in the IR and integrate up to the UV where we want our solutions to exhibit the appropriate behaviour. To accomplish this one needs the IR- and UV-asymptotics of the metric functions and the dilaton. They have been derived in [23],[29] and we present the results in Appendix B.

So our numerical integration proceed as follows. Using the IR-asymptotics in the A-coordinate system we give boundary conditions deep in the IR(B.15),(B.18). Then we integrate up to the UV where we want to check their behaviour with the UV asymptotics in the A-coordinate. As the UV-asymptotics come with the integration constant Λ it is vital to set its value. This can be achieved by using the UV-expansions through which one can show that

$$\hat{A} = \ln(\mathcal{L}_0 \Lambda) = \lim_{A\to\infty} (A - \frac{1}{b_0 \lambda(A)} + \frac{b_1}{b_0^2} \ln(b_0 \lambda_2(A)). \tag{5.11}$$

We will now set $\Lambda = 1$ in the rest of the calculation so this amounts to the rescaling $A_1(A) = A - \hat{A}$. All the solutions with this shifted coordinate A_1 have the required asymptotics and as the Einstein equations are invariant under coordinate shifts of A we acquire new solutions to them, albeit with different

boundary conditions. As it turns out the convergence of (5.11) is rather slow due to the $\mathcal{O}(\lambda) = \mathcal{O}(A^{-1})$ corrections so we have to speed it up by considering a form which eliminates those corrections:

$$\hat{A}_{Imp}(A_{max}) = \hat{A}(A_{max}) - \hat{A}(A_{max})\frac{\lambda(A_{max})}{\lambda'(A_{max})}. \tag{5.12}$$

Now the shift will be done using this improved shift value instead of (5.11). This way we arrive at the final form of our solutions satisfying both the required UV and IR asymptotics.

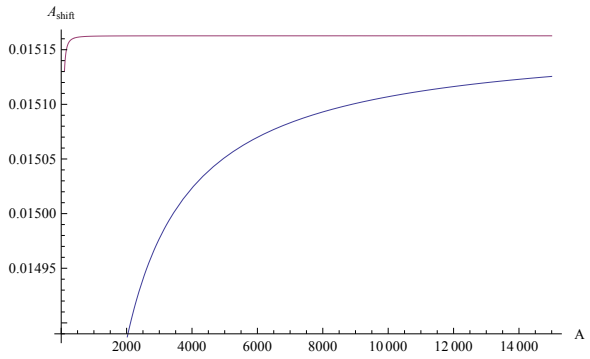

Figure 20: The required shift of the scale factor in order to set Λ to one as a function of A_{max}. The red curve is the "improved version" which converges substantially quicker to the correct value.

The Result

The construction of the background solution proceeded under the following considerations. Firstly, as stated before, the dilaton potential used will be "Potential II" of the form:

$$V_g(\lambda) = 12\Big(1 + \frac{88}{27}\lambda(A) + \frac{4619\lambda(A)^2\sqrt{1+\ln\big(1+\lambda(A)\big)}}{729\big(1+\lambda(A)\big)^{(2/3)}}\Big). \tag{5.13}$$

Additionally the integration constant R in the IR expansion and the AdS radius $\mathcal{L}_0$ are taken equal to one in our code. The IR integation constant will be set appropriately once the shift $\hat{A}_{Imp}$ has been done and all the dimensionful parameters are in units of the AdS-radius.

The resulting solutions are presented in Figure (11) where we see the required behaviour:

$$q(A_{max}) \approx -\mathcal{L}_0 \quad \text{and} \tag{5.14}$$

$$\lambda(A_{max}) \approx 0. \tag{5.15}$$

Finally the two shifts are displayed in the same figure in order to demonstrate the quicker convergence of (5.12).

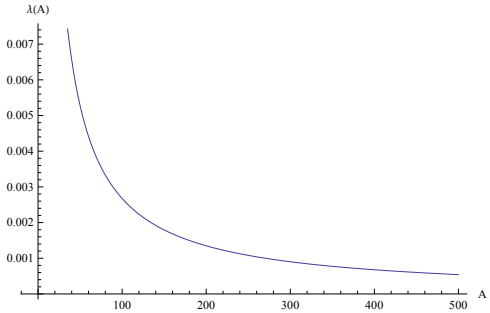

(a) The dilaton λ as a function of the scale factor A.

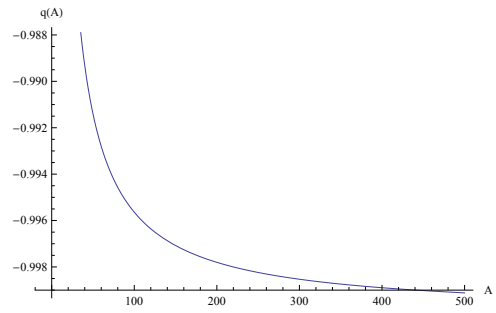

(b) The transformation function q as a function of the scale factor A.

Figure 21

5.2.2 Solving the Tachyon

Solving the Tachyon eom proceeds initially in a similar fashion as in the construction of the background. One sets boundary conditions at an IR-cutoff by using the IR-expansion of the tachyon (7.21) and integrates, in the presence of the previously constructed background, towards the deep UV where the appropriate behaviour should be demanded.

As shown in Appendix B the UV-behaviour of the tachyon is given by

$$\frac{1}{\mathcal{L}_0}\tau(r) = m_q r(-\ln(r\Lambda))^{-\gamma_0/b_0}\Big[1+\mathcal{O}\Big(\frac{1}{\ln(r\Lambda)}\Big)\Big] \tag{5.16}$$

$$+\,\sigma r^3(-\ln(r\Lambda))^{\gamma_0/b_0}\Big[1+\mathcal{O}\Big(\frac{1}{\ln(r\Lambda)}\Big)\Big], \tag{5.17}$$

with $\Lambda = 1$ as demanded during the construction of the background. Once a solution of the tachyon is constructed it is possible to get the corresponding bare quark mass by the following relation, constructed from the UV-expansions:

$$m_q = \lim_{A\to\infty} \mathcal{L}_0\tau(A)\exp\Big[\frac{1}{b_0\lambda(A)} + \Big(\frac{b_1}{b_0^2} - \frac{9}{22}\Big)\ln(b_0\lambda(A))\Big]. \tag{5.18}$$

In practice we will introduce two cutoff values of A and extrapolate to $\lambda = 0$ in order to achieve the extrapolation to $A = \infty$. The corresponding expression for the mass then becomes

$$m_q = \frac{\tilde{m}_q(A_1)\lambda(A_2) - \tilde{m}_q(A_2)\lambda(A_1)}{\lambda(A_2) - \lambda(A_1)}. \tag{5.19}$$

Now for a $m_q = 0$ tachyon solution the condensate can be calculated in a similar fashion as above. One takes the UV-expansion of the tachyon without mass

$$\frac{\tau(r)}{\mathcal{L}_0} = \sigma r^3(-\ln(\Lambda r))^{3/2b_0} \tag{5.20}$$

and

$$A - \ln(\Lambda \mathcal{L}_0) = \frac{1}{b_0 \lambda(A)} + \frac{b_1}{b_0^2} \ln(b_0 \lambda(A)) = \ln(\Lambda r),\ A \to \infty \tag{5.21}$$

and combine them in an appropriate way to obtain

$$\ln \tilde{\sigma}(A) = \ln \tau(A) - \ln \mathcal{L}_0 + \frac{3}{b_0 \lambda(A)} + \frac{3b_1}{b_0^2} \ln\big(b_0 \lambda(A)\big) + \frac{3}{2b_0} \ln\big(b_0 \lambda(A)\big) \tag{5.22}$$

which approaches $\ln \sigma$ for $A \to \infty$. Thus one can determine the chiral condensate value at a large enough cutoff.

Up till now we have not considered any limitations of the code. These limitations come into play when fixing the bare quark mass term. As we shoot from the IR the final solution cannot have vanishing mass but will always retain a tiny value. This is a result coming from fixing the IR boundary conditions which cannot be fine tuned beyond the numerical accuracy of the code. Now the linear term will dominate over the cubic term in the deep UV where one needs to separate the two contributions. As a correct value for the condensate requires a large UV cutoff of the order of $A \approx$hundreds, direct separation requires a numerical accuracy of $e^{-\text{hundreds}}$ which is impossible to achieve. Hence a workaround must be constructed.

Now a method in order to construct the desired tachyon solution with zero bare quark mass was proposed by Kiritsis et. al in [27]. The idea is to integrate from the IR and acquire a solution with the minimal possible mass. This will fix, up to a certain accuracy, the IR constant T_0. Once this value is determined we impose zero mass by shooting from the boundary with the initial conditions

$$\tau(r) = e^{-3A}, \quad \tau'(r) = -3e^{-3A}. \tag{5.23}$$

In the IR the tachyon will behave as $\tau(IR)$ times a constant and thus we can obtain this constant. One then normalises the solution gotten by shooting from the UV with this constant and obtains the true solution which, in the IR, coincides with the solution constructed by shooting from the IR and in the UV shows a zero bare quark mass behaviour.

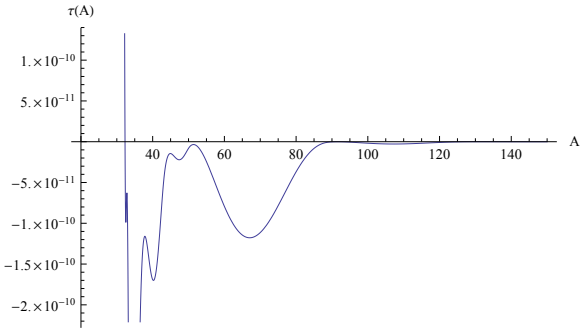

Figure 22: A typical tachyon behaviour generated by our code. The Efimov vacua are very clear.

The Result

Using the above presciription the tachyon eom in the A-coordinates (A.6) was solved with the potentials $V_f(\tau,\lambda), \kappa(\lambda)$ and $w(\lambda)$ as defined in (4.39) for $W_0 = \frac{3}{11}$. This choice for W_0 comes from the Veneziano QCD results as in this limit this choice yields a quantitatively correct finite T phase diagram of QCD [26],[27],[28].

Unfortunately the tachyon solutions acquired, within the range accesable by our processor, never managed to give the desired results. A typical behaviour is presented in Figure 12. As it is clear the tachyon has multiple roots before going to zero in the UV. These nodes are typically associated with Efimov vacua and according to [26],[27], correspond to solutions which have a higher free energy than the solutions with the same bare quark mass and no nodes. Additionally when considering the zero mass case the trivial solution would be dominant over the solutions with nodes. Hence we do not observe any chiral symmetry breaking with these solutions. Now increasing the value of the constant T_0 in the IR gives solutions with decreasing amounts of nodes but, as there is a maximum beyond which numerical errors appear, we are not able to reach a high enough value. Thus, in order to study this system further, an improvement in our processing power is required.

6 Discussion

During this project we studied the influence of an external magnetic field on the formation of a chiral condensate, signifying spontaneous chiral symmetry breaking. In the case of the AdS-Soliton a high-precision dependence of the condensate on the magnetic field was constructed and presented. The magnetic field enhanced the condensate hence we observed magnetic catalysis. As Lattice QCD predicts the appearance of inverse magnetic catalysis it should be part of a consistent holographic model of QCD. The fact it is not present in the AdS-Soliton model can be attributed to two aspects. Firstly the AdS-Soliton is still a rather crude approximation of QCD, a problem potentially solved by IHQCD. Secondly the addition of flavour was done in the quenched approximation. It might be the fact that only a fully backreacting tachyon in the Veneziano limit can encorporate the inverse magnetic catalysis phenomenon. This would require abandoning the background solutions and resolving the gravity system with a backreacting tachyon and magnetic field.

Now in the case of IHQCD enhanced with flavour degrees of freedom in the quenched approximation it was not possible to construct chiral symmetry breaking solutions in order to study (inverse) magnetic catalysis. It was only possible to construct tachyon solutions containing multiple Efimov vacua as above a certain value of the tachyon boundary constant T_0 the mathematica code refused to work. The reasons for this behaviour is expected to be purely numeric. Up till this moment no mistakes in the set-up have been found so additional subtle numeric techniques combined with substantially increase in processing power seems to be the solution to this.

7 Outlook

This subject, broad as it is, welcomes many extensions and improvements. Firstly, when considering the case of IHQCD, one needs to improve the numerical aspect of the work. This would definitely require additional processing power as the AMD Phenom II X2 processor these calculations were done on shows severe limitations. As it seems, at least a multicore Intel Core i7 is needed in order to overcome the Efimov vacua regime and to be able to accurately measure the condensate.

When one manages to successfully resolve the IHQCD+flavour in the quenched approximation system it is natural to consider different regimes. This will imply taking the Veneziano limit, hence χ_f finite. This has already been studied for finite temperature and/or finite density by Kiritsis, Järvinen et al [28],[27], [29]. Besides the chirally broken phase in the confining background they discovered that, for finite density, a chiral symmetry breaking phase exists in the deconfined phase as well. This would be an extremely interesting regime to study the effect of the magnetic field on the chiral condensate . In order to probe the chirally broken phase in the deconfining background a baryon density is required. To achieve its addition a nonzero time-component of the gauge-field in the bulk must be introduced as its dual. Once this is successfully done a very powerful dual theory to QCD will have been constructed. Therefore non-perturbative observables of QCD must be calculated in order to put the theory to the test.

Turning to the AdS-Soliton model, a similar generalization as above is natural. First one would need to abandon the quenched approximation in favour of the Veneziano limit. This might bring an additional number of subtleties with it which, up to this point, have not been studied but could potentially resolve the issue of the missing inverse magnetic catalysis regime. Once a successful Veneziano limit has been constructed a density can be added. Interesting as this might be, the original limitations of the model will remain and thus a complete dual description of QCD is improbable.

Acknowledgements

First and foremost, i would like to thank Umut for his guidance and encouragement during the course of this project. Second, without the help of my friend and fellow student, Alex, this project would have never reached the point it did. This work was a tight collaboration consisting of endless hours of discussion and back to back work as the worn out chairs in the masters' room can testify. Also i would like to thank Olga, Tara, Aron and Panos for the discussions. Special thanks also to Ioannis Iatrakis and Matti Järvinen for their speedy advice when the project called for it. This period of my life was heavily influenced by my friends, both in the Netherlands and in Greece, whom i thank for all the good times we shared. I would especially like to thank Lefteris for his utmost belief in my capabilities and the prospect of a Nobel prize in my future. Last, but not least, i am eternally grateful for the love, support and friendship my family has given me all these years.

Appendices

A A-Coordinate System

The equations (4.41), (4.46) encapture the dynamics of the Einstein Dilaton system cobined with a non-backreacting tachyon and magnetic field. As advocated before, to explore spontaneous chiral symmetry breaking it is necessary to restrict ourselves to $m_q = 0$. This is a technically demanding task forcing the solution to extend deep into the UV to extremely small $r \approx e^{-A}$, up to $A \sim$ hundreds. Hence, numerically it is a drastic improvement to consider our system by using the scale factor A as a coordinate.

The change of basis is achieved through the relation:

$$q(A) = e^A \frac{dr}{dA}. \tag{A.1}$$

After applying the above relation the system of Einstein equations becomes:

$$-3\frac{q'}{q} = -\frac{4}{3}\frac{\lambda'^2}{\lambda^2} \tag{A.2}$$

$$f'' + f'(4 - \frac{q'}{q}) = 0 \tag{A.3}$$

$$12f + 3f' - f\frac{4}{3}\frac{\lambda'^2}{\lambda^2} = V_g q^2. \tag{A.4}$$

The corresponding scalar equation becomes:

$$\frac{8}{3}f\Big(\frac{\lambda'}{\lambda} + \frac{\lambda''}{\lambda} - \frac{\lambda' q'}{\lambda q}\Big) + \frac{f'\lambda'}{\lambda} + \frac{3f\lambda'}{\lambda} = -q^2\partial_\lambda V_g \tag{A.5}$$

and finally the tachyon EOM is:

$$\begin{aligned}\tau''(A) = &+ \frac{\partial_\tau \ln V_f}{\kappa}\Big(q^2/f + (\tau')^2\kappa\Big) \\ &- (\tau')^3\frac{\kappa}{q}f\Big(\frac{f'}{2f} + \frac{\lambda'}{2}\partial_\lambda \ln(V_f^2\kappa) + \frac{1}{2}\frac{8e^{8A} + B^2we^{4A}(4w + 2\lambda'\partial_\lambda w)}{e^{8A} + B^2w^2e^{4A}}\Big) \\ &+ \tau'\Big(2 + \frac{f'}{2f} - q' + \frac{2e^{8A}}{e^{8A} + B^2w^2e^{4A}} + \lambda'\partial_\lambda \ln(V_f\kappa) + \frac{\lambda' B^2e^{4A}w^2\partial_\lambda \ln w}{e^{8A} + B^2w^2e^{4A}}\Big)\end{aligned} \tag{A.6}$$

B UV and IR Asymptotics of IHQCD With Flavour Degrees of Freedom

B.1 The UV-Structure

B.1.1 The Background

The equations of motion will be the system (4.41) with $f = 1$ and the dilaton potential taken in its UV-asymptotic form:

$$V_g(\lambda) = \frac{12}{\mathcal{L}_0}(1 + V_1\lambda + V_2\lambda^2 + ...), \tag{B.1}$$

where

$$V_1 = \frac{8}{9}b_0 = \frac{88}{216\pi^2} \tag{B.2}$$

$$\frac{V_2}{V_1^2} = \frac{23}{64} + \frac{9b_1}{16b_0^2} = \frac{1}{64}\Big(23 + \frac{54\times 34}{11}\Big). \tag{B.3}$$

Then, by plugging in suitable ansatzë, we obtain the leading order behaviour of the scale factor and the dilaton:

$$A(r) = -\ln\frac{r}{\mathcal{L}_0} + \frac{4}{9\ln(r\Lambda)} \tag{B.4}$$
$$+ \frac{1/162\Big[95 - \frac{64V_2}{V_1^2}\Big] + 1/81\ln(r\Lambda)\Big[-23 + \frac{64V_2}{V_1^2}\Big]}{\ln(r\Lambda)^2} + \mathcal{O}\Big(\frac{1}{\ln(r\Lambda)^3}\Big)$$

$$V_1\lambda(r) = -\frac{8}{9\ln(r\Lambda)} + \frac{\ln[-\ln(r\Lambda)]\Big[\frac{46}{81} - \frac{128V_2}{81V_1^2}\Big]}{\ln(r\Lambda)^2} + \mathcal{O}\Big(\frac{1}{\ln(r\Lambda)^3}\Big) \tag{B.5}$$

B.1.2 The Tachyon

Once we have obtained the leading order UV-asymptotic form of the background funtions we can plug them into the tachyon eom together with the asymptotic form of the fermionic potential:

$$\kappa = 1 + \kappa_1\lambda + \kappa_2\lambda^2. \tag{B.6}$$

As it turns out the magnetic field only affects the tachyon subleadingly and hence we obtain the zero magnetic field case[29]:

$$\frac{1}{\mathcal{L}_0}\tau(r) = m_q r(-\ln(r\Lambda))^{-\gamma_0/b_0}\Big[1 + \mathcal{O}\Big(\frac{1}{\ln(r\Lambda)}\Big)\Big] \tag{B.7}$$
$$+ \sigma r^3(-\ln(r\Lambda))^{\gamma_0/b_0}\Big[1 + \mathcal{O}\Big(\frac{1}{\ln(r\Lambda)}\Big)\Big] \tag{B.8}$$

with the perturbative anomalous dimension of the quark mass in QCD giving

$$\frac{\gamma_0}{b_0} = \frac{9}{22}. \tag{B.9}$$

B.2 The IR Structure

In the case of the IR-asymptotics the magnetic field affects once again only the subleading part hence we can proceed by neglecting its influence.

B.2.1 The Background

The asymptotic for of our dilaton potential now takes the form

$$V_g(\lambda) = u_0\lambda^{4/3}\sqrt{\ln\lambda}\Big[1+\frac{u_1}{\ln\lambda}+\frac{u_2}{\ln^2\lambda}\Big]. \tag{B.10}$$

Following the usual methodology one arrives at the following asymptotic forms:

$$\begin{aligned} A =& -\frac{r^2}{R^2}+\frac{1}{2}\ln\frac{r}{R}-\ln R-\frac{1}{2}\ln u_0+\frac{5}{4}\ln 2+\frac{3}{4}\ln 3+\frac{23}{24}+\frac{4u_1}{3} \\ &+\frac{R^2(-173+512u_1^2+1024u_2)}{3456r^2}+\mathcal{O}(r^{-4}) \end{aligned} \tag{B.11}$$

$$\ln\lambda = \frac{3}{2}\frac{r^2}{R^2}-\frac{23}{16}-2u_1-\frac{R^2(151+512u_1^2+1024u_2)}{2304r^2}+\mathcal{O}(r^{-4}) \tag{B.12}$$

with R an integration constant and the remaining constants being :

$$u_0 = \frac{12\times 4619}{729\mathcal{L}_0^2} = \frac{18476}{243} \tag{B.13}$$

$$u_1 = \frac{1}{2}, \qquad u_2 = -\frac{1}{8}. \tag{B.14}$$

As the integration proceeds in the A-Coordinate system it is appropriate to give the IR asymptotics in these coordinates as well. The expansion of the radial coordinate and the dilaton in terms of the scale factor now becomes:

$$\begin{aligned} \frac{r^2}{R^2} =& -A+\frac{1}{4}\ln(-\frac{3}{2}A)+A_0+\frac{23}{24}+\frac{4u_1}{3} \\ &-\frac{655+1152u_1+512u_1^2+1024u_2}{3456A}-\frac{\ln(-\frac{3}{2}A)+12A_0}{16A}+\mathcal{O}(A^{-2}) \end{aligned} \tag{B.15}$$

$$\ln\lambda = -\frac{3}{2}A+\frac{3}{8}\ln(-\frac{3}{2}A)+\frac{3}{2}A_0-\frac{7+16u_1+3\ln(-\frac{3}{2}A)+12A_0}{32A}+\mathcal{O}(A^{-2}). \tag{B.16}$$

The new function,$q(A)$, which encodes the transformation from the one coordinate system to the other can be expressed as:

$$q(A) = e^A r'(A) \tag{B.17}$$

and thus becomes:

$$q(A) = -\frac{R}{2}e^A(-A)^{-1/2}\Big[1+\frac{1}{8A}\Big(\ln(-\frac{3}{2}A)+4A_0+\frac{9}{2}+\mathcal{O}(A^{-2})\Big)\Big] \tag{B.18}$$

$$\lambda(A) = e^{-\frac{3}{2}(A-A_0)}(-\frac{3}{2}A)^{3/8}\Big[1-\frac{3}{32A}\Big(\ln(-\frac{3}{2}A)+4A_0+5\Big)+\mathcal{O}(A^{-2})\Big]. \tag{B.19}$$

Above we also gave the asymptotic expansion of $\lambda(A)$ as it is relevant for our numerics.

7.2.2 The Tachyon

Proceeding as usual one needs to plug the background expansions and the asymptotic form of the potentials into the tachyon eom and obtain the asymptotic form. As the magnetic field does not alter the leading form we will state the $B = 0$ result[29] which, for our potentials with the form

$$\alpha(\lambda) \approx \lambda^0; \quad \kappa(\lambda) \approx \lambda^{(4/3)}; \quad V_{f0}(\lambda) \approx \lambda^2 \tag{7.20}$$

becomes

$$\tau \approx e^{C_I r/R} \approx e^{C_I \sqrt{-A}} \tag{7.21}$$

whith the coefficient being a combination of known constants and the powers of lambda in the potentials

$$C_I = \frac{81 3^{5/6} 11 5^{4/3} 11}{8129442^{1/6}}. \tag{7.22}$$

The tachyon diverges for $r \to \infty, A \to -\infty$ as it should.

References

[1] M.E. Peskin, D.V. Schroeder, *"An Introduction to Quantum Field Theory"*, Addison-Wesley, Reading, 1995.

[2] J. Maldacena, *"The Large N Limit of Superconformal Field Theories and Supergravity"*, Adv. Theor. Math. Phys. 2:231-252(1998), arXiv:hep-th/9711200v3.

[3] E. Witten, *"Anti-de Sitter Space, Thermal Phase Transition, And Confinement in Gauge Theories"*, Adv. Theor. Math. Phys. 2: 505-532 (1998), arXiv:hep-th/9803131

[4] I.A. Shovkovy, *"Magnetic Catalysis: A Review"*, (2012), arXiv:1207.5081v2 [hep-th]

[5] J. Polchinski, *"Dirichlet Branes and Ramond-Ramond Charges"*, Phys. Rev. Lett. **75**, 4724, arXiv:hep-th/9510017

[6] K.G. Wilson, *"Confinement of quarks"*, Phys. Rev. D 10 (1974), 2445.

[7] M. Creutz, *"Gauge Fixing, the Transfer Matrix and Confinement on a Lattice"*, Phys. Rev. D 15 (1977) 1128.

[8] G. Boyd et al., *"Thermodynamics of SU(3) Lattice Gauge Theory"*, Nucl. Phys. **B469**, (1996) 419-444, arXiv:hep-lat/9602007v1

[9] G.S. Bali, F. Bruckmann, M. Constantinou, M. Costa, G. Endrődi, Z. Fodor, S.D. Katz, S. Krieg, H. Panagoloupos, A. Schäfer, K. Szabó, *"Thermodynamic Properties of QCD in External Magnetic Fields"*, (2013), arXiv:1301:5826v1 [hep-lat]
G.S. Bali, F. Bruckmann, G. Endrődi, S.D. Katz, A. Schäfer, *"The QCD Equation of State in a Background Magnetic Field"*, (2013), arXiv:1406.0269v1 [hep-lat]

[10] M. Panero, *"Thermodynamics of the QDC Plasma and the Large-N limit", Phys.Rev.Lett.* ***103*** *(2009), arXiv:0907.3719v2 [hep-lat]*

[11] F. Karsch, *"Lattice QCD at High Temperature and Density"*, Lect. Notes Phys. **583** (2002) arXiv:hep-lat/0106019

[12] G. 't Hooft, *"Dimensional Reduction in Quantum Gravity"*, THU-93/26 (1993), arXiv:gr-qc/9310026v2

[13] L. Susskind, *"The World as a Hologram"*, J. Math. Phys. 36: 6377-6396 (1995), arXiv:hep-th/9409089

[14] G. 't Hooft, *"A Planar Diagram Theory for Strong Interaction"*, Nucl. Phys. **B72**, (1974), 461

[15] J. Casalderrey-Solana, H. Liu, D. Mateos, K. Rajagopal, U.A. Wiedemann, *"Gauge/String Duality, Hot QCD and Heavy Ion Collisions"*,(2012), arXiv:1101:0618v2[hep-th]

[16] H. Nastase, *"Introduction to AdS/CFT"*, (2007), arXiv:0712:0689v2 [hep-th]

[17] A. Karch, E. Katz, *"Adding flavour to AdS/CFT"*, JHEP **0206** (2002) 043, arXiV:hep-th/0205236v2

[18] A. Sen, *"Dirac-Born-Infeld Action on the Tachyon Kink and Vortex"*, Phys. Rev. D. **68**, 066008 (2003), arXiv:hep-th/0303057

[19] G. Gibbons, S.W. Hawking, *"Action Integrals and Partition Functions in Quantum Gravity"*, Phy. Rev. D. **15** (10): 2752

[20] J. Polchinksi, M.J. Strassler, *"Hard Scattering and Gauge/String Duality"*, Phys. Rev. Lett, **88** (2002) 031601, arXiv:hep-th/0109174"

[21] S.S. Gubser, A. Nellore, *"Mimicking the QCD equation of state with a dual black hole", ArXiv:0804.0434[hep-th]*

[22] U.Gürsoy, E. Kiritsis, L. Mazzanti, F. Nitti, *"Deconfinement and Gluon Plasma Dynamics in Improved Holographic QCD"*, Phys. Rev. Lett. **101**, 181601 (2008), arXiv:0804:0899[hep-th]

[23] U. Gürsoy, E. Kiritsis, *"Exploring Improved Holographic Theories for QCD: Part I"*, JHEP **0802** (2008) 032, arXiv:0707.1324v3 [hep-th]
U. Gürsoy, E. Kiritsis, F. Nitti, *"Exploring Improved Holographic Theories for QCD: Part II"*, JHEP **0802** (2008) 019, arXiv:0707.1349v3 [hep-th]

[24] U. Gürsoy, E. Kiritsis, L. Mazzanti, F. Nitti, *"Improved Holographic Yang-Mills at Finite Temperature: Comparison with Data"*, Nucl. Phys **B820** (2010) 148-177, arXiv:0903.2859v3 [hep-th]

[25] U. Gürsoy, E. Kiritsis, L. Mazzanti, F. Nitti, *"Holography and Thermodynamics of 5D Dilaton-Gravity"*, JHEP **0905** 033, arXiv:0812:0792v2 [hep-th]

[26] M. Järvinen, E. Kiritsis, *"Holographic Models for QCD in the Veneziano Limit"*, JHEP, **1203** (2012) 002, arXiv:1112.1261v2 [hep-th]

[27] T. Alho, M. Järvinen, E. Kiritsis, K. Tuominen, *"On finite temperature holographic QCD in the Veneziano limit"*, (2012), arXiv:1210.4516v1[hep-th]

[28] T. Alho, M. Järvinen, K. Kajantie, E. Kiritsis, C.Rosen, K. Tuominen, *"A holographic model for QCD in the Veneziano limit at finie temperature and density"*, (2012), arXiv:1210.4516v1[hep-th]

[29] D. Arean, I. Iatrakis, M. Järvinen, E. Kiritsis, *"The Discontinuities of conformal transitions and mass spectra of V-QCD"*, JHEP **1311**, (2013) 068, arXiv:1309.2286 [hep-th]

[30] R. Casero, E. Kiritsis, A. Paredes, Nucl. Phys. **B787** (2007) 98-134, arXiv:070.2155v1 [hep-th]

[31] A.A. Tseytlin, *"On Non-Abelian Generalisation of the Born-Infeld Action in String Theory"*, Nucl. Phys. B **584**, 284 (2000), arXiv:hep-th/9701125

[32] I. Iatrakis, E. Kiritsis, A. Paredes, *"An AdS/QCD model from tachyon condensation: II"*, JHEP 1011, (2010) 123, arXiv:1010:1364 [hep-th].